✔ C-ペプチド

膵β細胞ではインスリン生合成の過程で前駆物質のプロインスリン1分子から生理活性を有するインスリン1分子と，生理活性を有さないC-ペプチド1分子が生じる．インスリンとC-ペプチドは1：1の割合で血中に分泌される．C-ペプチドは腎で代謝され約5％が尿中へ排泄される．そのため，24時間尿中のC-ペプチド排泄量を測定すれば1日の内因性インスリン分泌量を推定することができる．インスリン注射をしている患者の膵β細胞機能（インスリン分泌能）の評価にはインスリンのかわりにC-ペプチドを測定する．

詳しくいうと，膵β細胞でのインスリン生合成は，はじめに前駆体蛋白であるプレプロインスリンが作られ，小胞体内でプロインスリンとなる．プロインスリンは分泌顆粒内でプロホルモン変換酵素であるPC1/3，PC2などによる切断後カルボキシペプチダーゼE(CPE)による塩基性アミノ酸残基の除去を受け，インスリンA鎖とB鎖（ジスルフィル結合している）およびC鎖＝連結（connecting）ペプチドとなる（N末端側からB鎖，C鎖，A鎖の順）．この際はずれた連結ペプチドがC-ペプチドである．インスリンが1モル生成されればC-ペプチドも1モルできる．

✔ DCCT

1983～1989年に1型糖尿病患者を対象に米国とカナダで実施された多施設間大規模前向き臨床試験である（Diabetes Control and Complications Trial）．厳格な血糖コントロールが糖尿病性細小血管合併症の発症や進展を防止できることを初めて示したスタディである．従来インスリン療法と強化インスリン療法群の2群に無作為に割り付けたところ，強化インスリン療法では，従来療法に比較して細小血管障害の新たな発症や進展が有意に抑制され（発症の抑制は一次予防，進展の抑制は二次介入である），大血管障害のイベントも減少したと報告されている．

✔ HOMA-R

HOMA-R (homeostasis model assessment insulin-resistance)は，インスリン抵抗性の指標であり，5以上のときにインスリン抵抗性が示唆される．

HOMA-R＝空腹時血インスリン（μU/ml）×空腹時血糖（mg/dl）/405

この方法は肝臓からの糖の放出に対する内因性インスリンによる肝臓のインスリン感受性を反映しているとされる．ただし，軽度の耐糖能異常患者を対象にした簡便な指標であり，空腹時血糖＞150mg/dlの場合はこれを用いてインスリン抵抗性を評価することはむずかしい．インスリン分泌が低下している患者では，過小評価になりやすい．

✔ 緩徐進行1型糖尿病

1型糖尿病の典型例は，比較的急激に発症し，膵β細胞機能が廃絶するために発症早期よりインスリン依存性となる．これに対し，ICA，抗GAD抗体，IAA，抗IA-2抗体などの自己抗体が陽性で緩徐に発症する病型がある．すなわち，2型糖尿病（旧分類のインスリン非依存型糖尿病）と思われる糖尿病にも，自己抗体が陽性を示す例があり，発症・診断時は，インスリン非依存性であるが，平均3年で緩徐にインスリン分泌能が低下し，経口血糖降下薬の二次無効などをきたし最終的にはインスリン依存期に移行する．このような症例をslowly progressive IDDM (SPIDDM) とよぶ．

発症年齢は，30～60歳と中年から高齢であることが多く，急性発症の1型糖尿病と比べ高齢である．また，糖尿病の家族歴が高頻度である．

✔ [redacted]

UKPDS (United Kingdom Prospective Diabetes Study) は英国23施設で実施された無作為化前向き大規模臨床研究である．血糖や血圧コントロールと糖尿病合併症との関連を解析するために，1977年から1991年に新規に診断された2型糖尿病患者5102例を1997年まで追跡した．3ヵ月間の食事療法後に無作為に従来療法群（食事療法で開始しコントロールがつかないときは薬物療法を追加）とインスリン群，スルホニル尿素 (SU) 薬群，ビグアナイドのメトホルミン群（肥満者）などからなる強化療法群に割り付け，糖尿病に関連したエンドポイント（死亡，大血管症，細小血管症）の発症に差があるか否か検討された．治療法にかかわらず強化療法によるHbA_{1c}の低下によって合併症のリスクが軽減した．また血圧のコントロールによっても合併症のリスクが減少した．厳格な血糖コントロールや血圧コントロールが治療薬に関係なく糖尿病合併症発症リスクを減少させることが，2型糖尿病でも示された．

✔ [redacted]

インスリンの標的器官は，肝臓や筋肉，脂肪組織などであり，肝臓では糖の放出を抑制し，グリコーゲン合成を活性化して糖を取り込む．また，筋や脂肪組織では，糖輸送担体 (GLUT) 4を細胞内より細胞表面に移動させ，細胞内への糖輸送を活性化し，グリコーゲン合成を活性化する．さらに，インスリンは，脂肪代謝に関する酵素活性を調節する作用や，細胞内電解質濃度の調節作用なども有する．

インスリン抵抗性とは，糖代謝に対するインスリンの効果が発現しにくい状態をさし，健常人と同程度のインスリン作用を発揮するのに必要なインスリン量が，健常人よりはるかに上回る状態をいう．インスリン抵抗性の成因としては，インスリン作用の拮抗物質の存在や，インスリン標的細胞における受容体異常や受容体後過程の障害，などがあげられる．

2型糖尿病患者におけるインスリン抵抗性の多くは，脂肪細胞から分泌された腫瘍壊死因子α (TNFα)，FFA（遊離脂肪酸）や持続的な高血糖（糖毒性）が受容体後過程の障害をもたらしていることによる．インスリン抵抗性指数としてHOMA-Rがある (p.261参照)．

✔ [redacted]

チアゾリジン誘導体 (TZD：thiazolidinediones) は核内転写促進因子であるPPAR-γへの結合を介して脂肪細胞の分化・増殖や骨格筋での糖取り込みに関与する遺伝子の発現を調整することによりインスリン抵抗性を改善する．

TZDの一つであるトログリタゾン（ノスカール）は重篤な肝機能障害が生じたため発売中止となり，日本ではピオグリタゾン（アクトス）が唯一使用可能な薬剤である．欧米で発売されているロシグリタゾンも日本でも承認されるみこみである．

この薬剤の適応は，食事療法や運動療法では十分な効果は得られず，インスリン抵抗性が推定される場合，あるいはSU薬の効果が不十分な2型糖尿病である．肥満例やインスリン抵抗性指数が高い場合は有効性が高い，という報告もある．血糖降下作用のほか，中性脂肪低下作用やHDL-C（高比重リポ蛋白コレステロール）増加作用を有する．副作用として，浮腫や体重増加，心不全があり，心不全を合併する場合は禁忌で

ある．また，肝機能障害にも留意する必要があり，投与後1年間は月1回，肝機能検査が必要である．

✔ 熊本スタディ

熊本スタディは，中間型インスリン治療中の非肥満2型糖尿病患者110人を無作為に2群に割り付けて行われた．一群は中間型インスリン療法（従来療法群）を継続し，他群は頻回インスリン療法（強化療法群）に変更して8年間にわたって，血糖コントロール状態と細小血管合併症の累積悪化率を検討した．その結果インスリン頻回注射群では，網膜症ならびに腎症の悪化が有意に低く，合併症リスクが著明に軽減された．また，HbA_{1c}6.5%以下，空腹時血糖110mg/dl以下，食後2時間血糖180mg/dl以下に維持することが，細小血管合併症の発症，進展の阻止につながることが示された．

✔ グリセミック・インデックス

糖質摂取後の血糖の上昇の程度は種々の因子によって変わる．1981年Jenkinsらは標準食（ブドウ糖あるいはパン）と同じ量の糖質を含む食品を摂取した場合の血糖曲線と，標準食を摂取した場合の血糖曲線を比較してグリセミック・インデックス（GI：glycemic index）という概念を提唱した．グリセミック・インデックスは，食物繊維含量，糖質の種類（単純糖質か複合糖質か），脂肪含量，食品の形態，硬さ，消化酵素性阻害物質，消化管運動機能などに影響される．また，食品の調理法によっても指数が変化することも考えられるので，この数値を食事療法に応用して食事内容を設定し，食後高血糖の程度を予想することは困難である．

しかし，食品によっては血糖の上昇しにくいもの，あるいはブドウ糖と同程度の血糖上昇が認められる食品があることを認識することは必要であり，GIの低い食事が理想的である．

✔ 血糖自己測定

血糖自己測定（SMBG：self-monitoring blood glucose）とは，患者自身が血糖値を測定することである．その目的は，血糖値をリアルタイムに把握し，治療薬の投与量を適正化して良好な血糖管理を達成し，将来の合併症の出現や進展を予防することである．血糖自己測定は現在インスリン注射中の患者にのみ保険適用されており，その他の患者は自己負担で測定器を購入する必要がある．

適応を以下に示す．

① 1型糖尿病．
② インスリン注射中の2型糖尿病．
③ 糖尿病合併妊娠．
④ 手術前など厳格なコントロールが必要な患者．
⑤ 小児糖尿病．
⑥ インスリン持続皮下注入（CSII）療法中．

自己血糖測定器の測定原理としては，試験紙やセルなどの検出部にGOD（グルコース・オキシダーゼ）などの酵素を使用して反応過程を光学的に測定する酵素比色法と，電極を用いる酵素電極法とがある．測定器は採血時の痛みを軽減し，より使いやすく改良され，多種類が存在する．

なお，急激な血糖降下時には，前腕採血は測定値が手指での測定より遅れるという報告があり，低血糖時には注意が必要である．

✔ 抗GAD抗体

抗GAD抗体は1型糖尿病発症早期の患者に認められる．ヒト膵島細胞の蛋白（GAD）に対する自己抗体である．

グルタミン酸脱炭酸酵素（GAD）は神経伝達物質であるγ-アミノ酪酸（GABA）をグルタミン酸から合成する酵素で，分子量65kDa（キロダルトン）と67kDaの2種類が存在し，神経系や膵β細胞などに分布する．ヒト膵β細胞に主に存在するのは，65kDaのGAD65であり，IA-2とともにICA（膵ラ氏島抗体）の主な抗原となる．急性発症の自己免疫性1型糖尿病での発症早期の抗GAD抗体の陽性率は50～80％であり，HLA-DR3（組織適合抗原DR3型）陽性者に高率に認められる．ICAと異なり，陽性率が低下しにくい．抗GAD抗体は，1型糖尿病やSPIDDMのインスリン分泌不全が今後進展するかどうかの予知マーカーとして診断時に有用である．

✔

糖尿病患者が，かぜやインフルエンザなどの急性感染症，急性消化器疾患，外傷，急性ストレスなどを併発し，代謝失調を招いた状態をシックデイ（sick day）という．シックデイでは，インスリン抵抗性が高まりインスリン需要が増大することによる血糖の上昇，食事摂取不足による血糖の激しい変動や，食事摂取の低下に伴う脱水などがしばしば認められる．さらに脱水からケトーシスや昏睡が発症して救急対応が必要となることもある．特にインスリン治療中の患者では，経口摂取不能時のインスリン注射の中止によりケトアシドーシスをきたすことがある．そのためインスリン注射をやめないように十分な注意が必要である．シックデイには必ず受診するように，患者・家族に対してシックデイ指導を行う．持続する高血糖，尿ケトン体陽性，経口摂取不能，下痢，脱水や意識障害などが認められれば入院・加療が必要である．

✔

インスリン皮下注射をした後の血中への吸収をさらに速くしたのが超速効型インスリン（インスリンアナログ）である．日本イーライリリー社のインスリンリスプロ（ヒューマログ）とノボノルディスクファーマ社のインスリンアスパルト（ノボラピッド）がある．

従来の速効型インスリン製剤は，皮下からの吸収に時間がかかるため食前30分に注射する必要があったが，この新しい製剤により，食直前投与が可能となりインスリン患者の治療満足度やコンプライアンスを改善した．インスリンアナログの特徴は食後の高血糖を改善し，夜間の低血糖のリスクを減らすことである．

✔

糖尿病の罹病期間が長期にわたると，慢性合併症が発症・進展する．慢性合併症は，長期間持続する高血糖に起因する糖尿病代謝障害と血管障害によって起こる．三大合併症としては，糖尿病に特有である小動静脈や毛細血管に生じる細小血管合併症として知られている網膜症や腎症，ならびに神経障害があげられる．また，糖尿病をふくむ生活習慣病は，中大動脈に生じる動脈硬化症が発症・進展しやすく，冠動脈硬化症，脳血管障害，下肢閉塞性動脈硬化症などの大血管障害を合併することが多い．

✔ 糖尿病性昏睡

糖尿病性昏睡とは，広義には糖尿病患者が高血糖により意識障害をきたした場合である．

① 糖尿病性アシドーシスまたはケトン性昏睡，

② 高浸透圧性非ケトン性昏睡（HONC），

③ 乳酸アシドーシス，

の3つをさしている，しかし，臨床上鑑別すべきものは，低血糖昏睡，脳血管障害などの意識障害を呈する疾患がある．高浸透圧性非ケトン性昏睡ではケトン体の産生量は比較的少ない．糖尿病性昏睡は発症初期に適切な治療をするか否かが予後を決める．最近では2型糖尿病若年男性の清涼飲料水の多飲による糖尿病性ケトアシドーシス（ペットボトル症候群，ソフトドリンク・ケトーシス）もある．またUKPDSによりメトホルミンが再評価されているが，高齢者や腎・心機能低下のある患者ではメトホルミンによる乳酸アシドーシスの発症の報告があり，使用には注意が必要である．

✔ 糖尿病性ケトアシドーシス

糖尿病性ケトアシドーシス（DKA）は，インスリンの欠乏やインスリン拮抗ホルモンであるグルカゴン，カテコラミンなどの過剰により生ずる高度の代謝失調状態である．インスリン作用の極度の低下により，糖利用低下，脂肪分解の亢進が起こり，高血糖と高遊離脂肪酸血症を招く．遊離脂肪酸はインスリン欠乏下の肝では急速に酸化を受け，ケトン体を生ずる．高ケトン体血症が血液の緩衝作用を凌駕した結果発症したアシドーシスと脱水がDKAの本体であり，重症では昏睡になる．尿中や血中のケトン体が高値になるが，DKA時のケトン体の主要成分はアセト酢酸と3-ヒドロキシ酪酸で，特に後者が主体である．本病態は，1型糖尿病発症時のほか，1型糖尿病患者でインスリン注射を中断した場合，または，感染や重篤な全身性疾患などをきっかけとして起こる場合がほとんどである．2型糖尿病では清涼飲料水の過剰摂取によるケトアシドーシス（ペットボトル症候群，ソフトドリンク・ケトーシス）も認められることがある．

✔ 高浸透圧性非ケトン性昏睡（HONC）

HONCは脱水と高浸透圧が病態の中心であり，HONCにおけるインスリン欠乏は糖尿病性ケトアシドーシス（DKA）ほど著しくなく，ケトン体は正常から軽度増加にとどまっている．脳神経系の細胞内脱水と循環虚脱による脳の酸素不足により，意識障害が起こるとされ，その程度は血糖値よりも血漿浸透圧と相関する．一般に高血糖の程度はDKAに比べて著しく高く，血糖値は800mg/dl以上のことが多い．2型糖尿病の高齢者に多く，一般に回復後は良好な血糖コントロールに戻ることが多い．

✔ 内臓脂肪型肥満

肥満の分類についてはp.85を参照されたい．

動脈硬化発症の進展に関与する糖尿病・高血圧・高脂血症などの生活習慣病は，それぞれが重複して合併することが多い．各病態が重積した状態は，“シンドロームX”“インスリン抵抗性症候群”“内臓脂肪症候群”“マルチプル・リスクファクター・シンドローム”“メタボリック・シンドローム”などとよばれている．内臓脂肪型肥満は，これらの病態の成因の基盤の一つである．最近，脂肪組織は単なるエネルギーの貯蔵庫ではなく，活発に生理活性物質を分泌する臓器として認識されている．

内臓脂肪の分解により生じる遊離脂肪酸（FFA）は，門脈に流入することにより，肝臓でのインスリン取り込みを抑制したり，肝臓や筋肉でのインスリン抵抗性をきたす．また，脂肪組織より分泌される腫瘍壊死因子α（TNFα）もインスリン抵抗性を引き起こすといわれている．

✔ [illegible]

インスリン治療患者のなかでも日内・日差の（「一日のなかで」または「日ごとの」）血糖変動が大きく，低血糖と高血糖を頻回にくり返し，血糖が予想を超えた動揺を示す糖尿病のことである．ほとんどが1型糖尿病である．一般には，外来患者がある一定期間に頻回に測定した空腹時血糖値の標準偏差が80mg/dl以上の場合や，最高値と最低値の差が200mg/dl以上などの場合は，不安定型糖尿病と扱うことが多い．不安定型糖尿病の病因としては，内因性インスリン分泌の高度障害を基盤としており，これにグルカゴンやカテコラミンなどインスリンと拮抗するホルモン分泌の異常が重なるときに典型的な病像があらわれる．

✔ [illegible]

ブドウ糖負荷試験（OGTT）は，ブドウ糖を負荷して糖処理能を調べる検査であり，軽い糖代謝異常をみつけるための最も鋭敏な検査法である．糖質を150g以上含む食事を3日以上摂取した後，早朝空腹時にブドウ糖75gを250～350mlの溶液として経口負荷する．食事と食事の間の空腹状態の時間は10～14時間とし，検査終了までは水以外の摂取を禁止し，なるべく安静を保たせ，禁煙とする．

糖尿病の診断目的のためには，少なくとも負荷前と負荷後2時間目の血糖値を測定する．空腹時血糖値が126mg/dl以上，または75gOGTTの2時間血糖値が200mg/dl以上，いずれかが認められた場合は“糖尿病型”と判定し，もう一度OGTTをする．それが糖尿病型であれば糖尿病とする．

✔ [illegible]

高血糖ではグルコースが蛋白質と非酵素的に結合するグリケーションが促進することが知られ，この代表的なもので現在の糖尿病臨床で血糖コントロール指標としての意義を確立したものがヘモグロビン（Hb）A_{1c}である．過去1～2ヵ月の平均血糖値を反映する．基準値は4.3～5.8％であり，5.8～6.5％が糖尿病の血糖コントロールの評価では良であり，8.0％以上のときはなんらかの治療変更を考える必要があるとされている．

肝硬変や溶血性貧血，鉄欠乏性貧血の回復期，エリスロポエチンによる貧血の治療ののち，輸血などではHbA_{1c}は血糖値に比して低い値となり，血糖のコントロール状況を反映しない．これらの場合は血糖コントロールの指標としてHbA_{1c}よりもグリコアルブミンが適している．

✔ [illegible]

ペン型注射器は，ダイアル式携帯用インスリン注入器とよばれるものである．1988年から臨床応用され，携帯が便利で操作が簡単である．それに加えて，注射針も30G，31Gと細いため痛みが比較的弱い．そのため急速に普及し，多種多様のペン型注射器が発売されている．インスリン療法中の患者では欠かせないものになっている．

ペン型注射器にはカートリッジを装着するタイプとペン型の使い捨てタイプがあり，速効型や中間型，混

合型のものがある．1型小児糖尿病患者のための0.5単位ずつ刻めるもの（ノボペン300デミ）や，高齢者で視力の低下した患者でも，めもりがみやすくカートリッジの交換の必要のないインスリンキット製剤（イノレット300，ヒューマカートキット，フレックスペン）なども開発され，各々の患者に応じて最も適した製品を選択することができる．

✔ ミトコンドリア異常

糖尿病のなかには，一つの遺伝子が変異することによって起こる糖尿病もある．このようにして起こる糖尿病のうち最も高頻度なのは，ミトコンドリア遺伝子のDNA（mtDNA）の変異によって起こる糖尿病である．mtDNAが変異するとミトコンドリア機能異常をきたす．mtDNAの変異は母系遺伝し，その家系には，脳卒中様発作を伴うミトコンドリア脳筋症（MELAS），ミオクローヌスてんかん（MERRF），リーバー（Leber）病，ミトコンドリア心筋症，mtDNA欠失を伴う慢性進行性外眼筋麻痺（CPEO），キーンズ・セイアー（Kearns-Sayre）症候群などとともに，糖尿病がよく認められる．ミトコンドリア異常によって起こる糖尿病は，全糖尿病患者の約1％程度を占め，発病は20～30歳代で，インスリン分泌の低下とともに，感音性難聴も同時に発症する．

✔ レプチン

脂肪組織から分泌されるレプチンは，視床下部の満腹中枢に働き，摂食を抑制し，かつ交感神経系を活性化して，エネルギー代謝を調節して肥満を抑制する蛋白である．遺伝性肥満マウスである*ob/ob*マウスから単離された肥満遺伝子（*ob*遺伝子）より作られる分泌蛋白であり，ギリシア語の「やせる」意味の“*leptos*”にちなんでレプチンと命名された．肥満モデルマウス*ob/ob*マウスでは*ob*遺伝子変異によりレプチンの生物活性が低下し，肥満をきたすと考えられている．最近，著しい小児肥満患者にレプチン遺伝子変異が同定され，ヒトでもレプチンが重要なエネルギー代謝調節因子であることが明らかになった．レプチンは体脂肪率やBMIと良好な正相関をもつ．肥満患者では，一般的にレプチンは高値であるが，これはレプチンに対する抵抗性が存在することによると考えられている．

Increased oxidative stress in obesity and its impact on metabolic syndrome

Shigetada Furukawa,[1] Takuya Fujita,[1] Michio Shimabukuro,[2] Masanori Iwaki,[1] Yukio Yamada,[1] Yoshimitsu Nakajima,[3] Osamu Nakayama,[3] Makoto Makishima,[1] Morihiro Matsuda,[1] and Iichiro Shimomura[1,4,5]

[1]Department of Medicine and Pathophysiology, Graduate School of Medicine, Department of Organismal Biosystems, Graduate School of Frontier Biosciences, Osaka University, Suita, Osaka, Japan. [2]Second Department of Internal Medicine, University of the Ryukyus, Nishihara, Okinawa, Japan. [3]Exploratory Research Laboratories, Fujisawa Pharmaceutical Co., Tsukuba, Ibaraki, Japan. [4]PRESTO, Japan Science and Technology Corporation (JST), Kawaguchi, Saitama, Japan. [5]Department of Internal Medicine and Molecular Science, Graduate School of Medicine, Osaka University, Suita, Osaka, Japan.

Obesity is a principal causative factor in the development of metabolic syndrome. Here we report that increased oxidative stress in accumulated fat is an important pathogenic mechanism of obesity-associated metabolic syndrome. Fat accumulation correlated with systemic oxidative stress in humans and mice. Production of ROS increased selectively in adipose tissue of obese mice, accompanied by augmented expression of NADPH oxidase and decreased expression of antioxidative enzymes. In cultured adipocytes, elevated levels of fatty acids increased oxidative stress via NADPH oxidase activation, and oxidative stress caused dysregulated production of adipocytokines (fat-derived hormones), including adiponectin, plasminogen activator inhibitor-1, IL-6, and monocyte chemotactic protein-1. Finally, in obese mice, treatment with NADPH oxidase inhibitor reduced ROS production in adipose tissue, attenuated the dysregulation of adipocytokines, and improved diabetes, hyperlipidemia, and hepatic steatosis. Collectively, our results suggest that increased oxidative stress in accumulated fat is an early instigator of metabolic syndrome and that the redox state in adipose tissue is a potentially useful therapeutic target for obesity-associated metabolic syndrome.

Introduction

Multiple risk factor syndrome or metabolic syndrome (i.e., the coexistence of several risk factors for atherosclerosis, including hyperglycemia, dyslipidemia, and hypertension in the same individual) is a growing medical problem in industrialized countries (1–3). Obesity is the central and causal component in this syndrome (4–7), but the mechanistic role of obesity has not been fully elucidated.

Adipocytes produce a variety of biologically active molecules (4–9), collectively known as adipocytokines or adipokines, including plasminogen activator inhibitor-1 (PAI-1) (10), TNF-α (11, 12), resistin (13, 14), leptin (15–17), and adiponectin (18–21). Dysregulated production of these adipocytokines participates in the pathogenesis of obesity-associated metabolic syndrome. Increased production of PAI-1 and TNF-α from accumulated fat contribute to the development of thrombosis (10) and insulin resistance (11, 12), respectively, in obesity. In contrast, adiponectin exerts insulin-sensitizing (22–25) and anti-atherogenic effects (26–28), and hence a decrease in plasma adiponectin is causative for insulin resistance and atherosclerosis in obesity. However, the mechanisms by which fat accumulation leads to such dysregulation of adipocytokines have not been elucidated.

Oxidative stress plays critical roles in the pathogenesis of various diseases (29). In the diabetic condition, oxidative stress impairs glucose uptake in muscle and fat (30, 31) and decreases insulin secretion from pancreatic β cells (32). Increased oxidative stress also underlies the pathophysiology of hypertension (33) and atherosclerosis (34) by directly affecting vascular wall cells.

In the present study, we suggest that obesity per se may induce systemic oxidative stress and that increased oxidative stress in accumulated fat is, at least in part, the underlying cause of dysregulation of adipocytokines and development of metabolic syndrome. As an early instigator of obesity-associated metabolic syndrome, increased oxidative stress in accumulated fat should be an important target for the development of new therapies.

Results

Oxidative stress and plasma adiponectin levels in human obese subjects. To investigate whether oxidative stress is increased in obese subjects, we measured lipid peroxidation, a marker of oxidative injury, in nondiabetic human subjects. Lipid peroxidation, represented by plasma thiobarbituric acid reactive substance (TBARS) and urinary 8-epi-prostaglandin-F2α (8-epi-PGF2α), significantly correlated with BMI and waist circumference (Figure 1A). Plasma adiponectin levels correlated inversely with BMI and waist circumference (Figure 1A), as we reported previously (21). We also found significant inverse correlations between plasma adiponectin and plasma TBARS and between plasma adiponectin and urinary 8-epi-PGF2α (Figure 1B). These results of human studies allowed us to hypothesize that fat accumulation itself could increase systemic oxidative stress independent of hyperglycemia, and that increased oxidative stress in obesity might relate to the dysregulated production of adipocytokines.

Increased oxidative stress in plasma and white adipose tissue of KKAy mice. To determine whether fat accumulation is primarily involved in increased oxidative stress, we analyzed 7-week-old KKAy mice as a model of nondiabetic obesity, and 13-week-old KKAy mice as a model of diabetic obesity. KKAy mice exhibit severe obesity, hyperlipidemia, and insulin resistance. Compared with age-

Nonstandard abbreviations used: DIO, diet-induced obesity; DPI, diphenyleneiodonium; 8-epi-PGF2α, 8-epi-prostaglandin-F2α; GPx, glutathione peroxidase; MCP-1, monocyte chemotactic protein-1; NAC, *N*-acetyl cysteine; NBT, nitroblue tetrazolium; NOX, NADPH oxidase; PAI-1, plasminogen activator inhibitor-1; SOD, superoxide dismutase; TBARS, thiobarbituric acid reactive substance; TG, triglyceride; WAT, white adipose tissue.

Conflict of interest: The authors have declared that no conflict of interest exists.

Citation for this article: *J. Clin. Invest.* 114:1752–1761 (2004). doi:10.1172/JCI200421625.

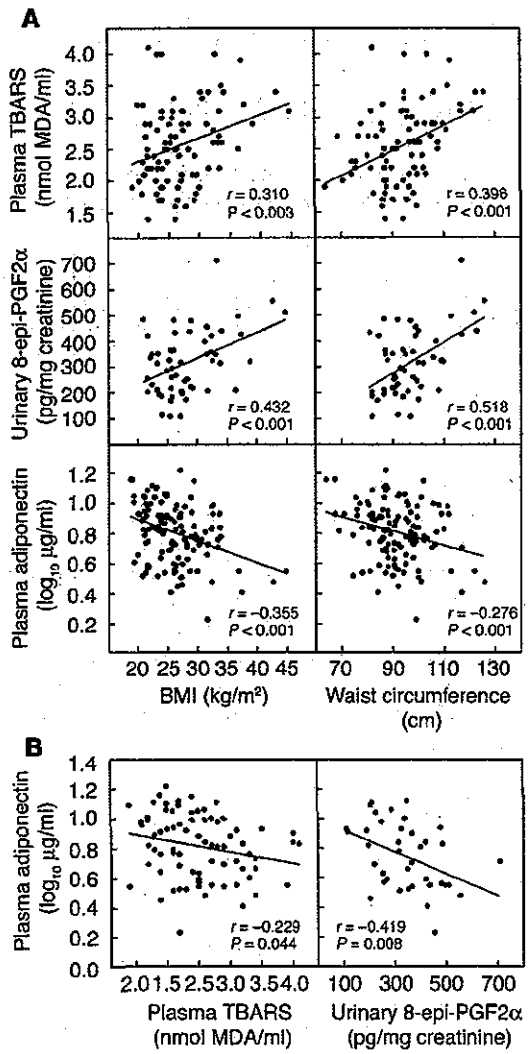

Figure 1
Levels of lipid peroxidation and plasma adiponectin in nondiabetic subjects. (**A**) Correlation of plasma TBARS, urinary 8-epi-PGF2α, and plasma adiponectin with BMI and waist circumference. (**B**) Correlation of plasma adiponectin with plasma TBARS and urinary 8-epi-PGF2α. Pearson's correlation coefficient (*r*) is shown for each relationship. MDA, malondialdehyde.

matched control C57BL/6 mice, KKAy mice at 7 and 13 weeks of age were significantly heavier (Figure 2A) and had a heavier parametrial fat pad (Figure 2A). The increase in plasma glucose was marginal in 7-week-old KKAy mice, but 13-week-old KKAy mice showed significant hyperglycemia relative to C57BL/6 mice (Figure 2A). Surprisingly, plasma lipid peroxidation in nondiabetic 7-week-old KKAy mice was significantly higher than in control mice, and was similar to that in diabetic 13-week-old KKAy mice (Figure 2A). Moreover, plasma levels of H_2O_2, a hazardous ROS against tissues and cells, were also elevated in nondiabetic and diabetic KKAy mice compared with C57BL/6 mice (Figure 2A). These results demonstrated that oxidative stress in blood was augmented in obesity, that is, fat accumulation, independent of hyperglycemia.

Next, we determined the tissue type that could be responsible for the increased oxidative stress in plasma of obese mice. Lipid peroxidation was markedly elevated in white adipose tissue (WAT) of 7- and 13-week-old KKAy mice compared with C57BL/6 mice (Figure 2B). In contrast, the levels of lipid peroxidation in the liver and skeletal muscle were similar between KKAy and C57BL/6 mice at both 7 and 13 weeks of age (Figure 2B). Furthermore, H_2O_2 production from WAT was significantly higher in 7-week-old KKAy mice than in the control mice (Figure 2C). In contrast, H_2O_2 production from skeletal muscle and aorta was not altered in KKAy mice (Figure 2C).

Similarly, plasma levels of lipid peroxidation were elevated in other mouse models of obesity, including the diet-induced obesity (DIO) model and another genetic model of obesity (*db/db* mice) (Supplemental Figure 1, A–D; supplemental material available at http://www.jci.org/cgi/content/full/114/12/1752/DC1). Similar increases in lipid peroxidation were observed in WAT, but not in the liver or skeletal muscle, of these obese mice (Supplemental Figure 1E). These results suggest that, in obesity, increased oxidative stress in plasma is due to increased ROS production from accumulated fat.

Dysregulated mRNA expressions of adipocytokines and PPARγ in WAT of KKAy mice. The mRNA expressions of adiponectin and PPARγ were lower in WAT of 7- and 13-week-old KKAy mice compared with C57BL/6 mice (Figure 3A). In contrast, the mRNA expressions of PAI-1 and TNF-α were high relative to the corresponding levels in the control mice (Figure 3A). We also found that plasma adiponectin levels were lower in KKAy mice than in C57BL/6 mice at both 7 and 13 weeks of age (19.7 ± 0.8 μg/ml vs. 26.2 ± 1.0 μg/ml, $P < 0.001$ at 7 weeks of age, 16.0 ± 0.9 μg/ml vs. 25.5 ± 1.8 μg/ml, $P < 0.001$ at 13 weeks of age). Thus, dysregulated expressions of adipocytokines already existed in the nondiabetic obese stage.

Increased mRNA expression of NADPH oxidase in WAT of KKAy mice. NADPH oxidase complex is a major source of ROS in various cells (35, 36). Increased NADPH oxidase activity in vascular cells has been reported to be important in the pathogenesis of hypertension and atherosclerosis by increasing oxidative stress (36). In order to investigate the possible role of augmented NADPH oxidase in increased ROS production, we determined the mRNA expression of NADPH oxidase in WAT of KKAy mice.

The NADPH oxidase complex consists of membrane-associated flavocytochrome b_{588} protein, which is composed of $gp91^{phox}$ and $p22^{phox}$, and cytosolic components $p47^{phox}$, $p67^{phox}$, and $p40^{phox}$. In C57BL/6 mice, the mRNA expression of each oxidase subunit was detected in WAT, and the expression levels of most subunits were quite high in WAT compared with other tissues tested (Figure 3B). The mRNA expression levels of these NADPH oxidase subunits were significantly augmented in WAT of nondiabetic 7-week-old KKAy mice, and they were even higher in WAT of diabetic 13-week-old KKAy mice compared with the control mice (Figure 3C). In contrast, the mRNA expression levels of these subunits in the liver and skeletal muscle of 7- and 13-week-old KKAy mice were similar to those of control mice (Figure 3D). We also found that the mRNA expression level of transcription factor PU.1, which is known to upregulate the transcription of NADPH oxidase subunits in myeloid cells (37), was also elevated in WAT (Figure 3C), but not in the liver or in skeletal muscle (Figure 3D) of KKAy mice compared with C57BL/6 mice. Similar mRNA changes of NADPH oxidase subunits were observed in WAT, but not in liver or skeletal muscle, of both DIO and *db/db* mice (Supplemental Figure 1, F and G). These results indicate that the NADPH oxidase pathway is specifically induced in WAT of obese mice.

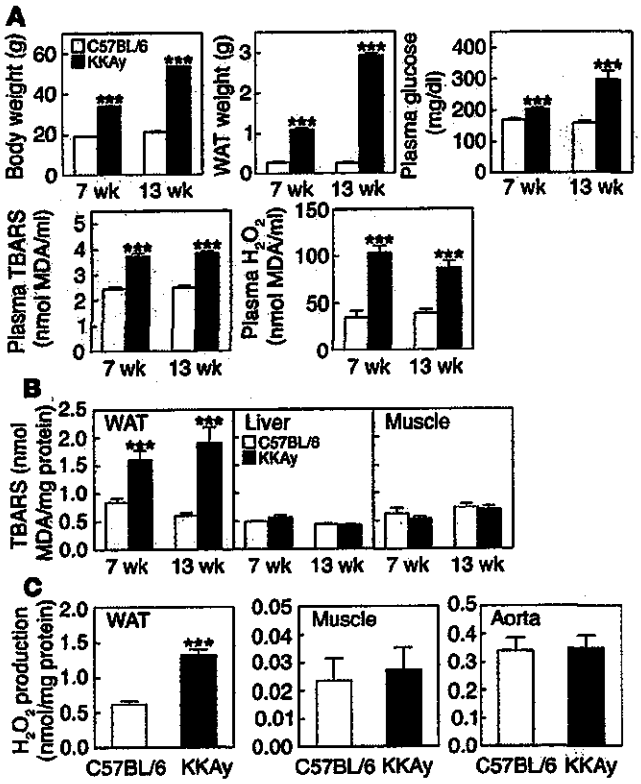

Figure 2
Increased oxidative stress in plasma and WAT of obese KKAy mice. (**A**) Body weight, parametrial WAT weight, plasma levels of glucose, lipid peroxidation (TBARS), and H_2O_2 in C57BL/6 and KKAy mice at 7 and 13 weeks of age. Values are expressed as mean ± SEM (n = 6–8). (**B**) Tissue levels of lipid peroxidation in WAT, liver, and skeletal muscle of C57BL/6 and KKAy mice. Values are expressed as mean ± SEM (n = 6–8). (**C**) The release of H_2O_2 from WAT, skeletal muscle, and aorta of C57BL/6 and KKAy mice at 7 weeks of age. Values are expressed as mean ± SEM (n = 5). ***P < 0.001 compared with C57BL/6 mice.

Decreased mRNA expressions and activities of antioxidant enzymes in WAT of KKAy mice. In the next step, we measured the expressions of antioxidant enzymes including superoxide dismutase (SOD), glutathione peroxidase (GPx), and catalase. At 7 weeks of age, the mRNA expression levels of cytoplasmic Cu,Zn-SOD, GPx, and catalase were significantly lower in WAT of KKAy mice, compared with C57BL/6 mice (Figure 4A). The expressions of Cu,Zn-SOD and catalase were also lower in WAT of 13-week-old KKAy mice, compared with C57BL/6 mice (Figure 4A). In contrast, the mRNA expression levels of these antioxidant enzymes in the liver and skeletal muscle of KKAy mice were similar to those of C57BL/6 mice (Figure 4A). The amount of Cu,Zn-SOD protein was also lower in WAT, but not in the liver and skeletal muscle, of KKAy mice compared with C57BL/6 mice (Figure 4B). Furthermore, total SOD activities (Figure 4C, left) and GPx activities (Figure 4C, right) were also significantly and specifically lower in WAT of KKAy mice than in the control mice. Similar mRNA decreases of Cu,Zn-SOD and GPx were observed in WAT, but not in liver or skeletal muscle, of DIO and *db/db* mice (Supplemental Figure 1, F and G). Taken together, these results indicate that increased ROS production in accumulated fat is due to the activated NADPH oxidase pathway and impaired antioxidant defense system (Figure 4D).

ROS production in adipocytes. We next examined the significance of ROS in cultured adipocytes. ROS production was markedly increased during differentiation of 3T3-L1 cells into adipocytes (Figure 5A), suggesting that ROS production increases in parallel with fat accumulation in adipocytes. We then determined the cellular pathway involved in increased ROS production in mature adipocytes, including NADPH oxidase, xanthine oxidase (34), and mitochondria-mediated (38) pathways. ROS production in fully differentiated 3T3-L1 adipocytes was markedly suppressed by 2 structurally unrelated inhibitors of NADPH oxidase, diphenyleneiodonium (DPI) and apocynin, as well as the general antioxidant *N*-acetyl-cysteine (NAC) (Figure 5B). In contrast, ROS production in 3T3-L1 adipocytes was not suppressed by oxypurinol, an inhibitor of xanthine oxidase, rotenone, an inhibitor of mitochondrial electron transport chain complex I, or thenoyltrifluoroacetone, an inhibitor of complex II (Figure 5B). These results suggest that NADPH oxidase is the major source of ROS in adipocytes, and that augmented NADPH oxidase seems to contribute to increased ROS production in adipose tissue in obesity.

It has been reported that in cultured vascular cells, free fatty acids increase NADPH oxidase activity (39). In the next experiment, we investigated whether free fatty acids could induce ROS production in 3T3-L1 adipocytes. ROS production was significantly increased by incubation with linoleic acid (Figure 5B), as well as with other types of fatty acids such as oleic acid and arachidonic acid (data not shown). The effect of linoleic acid was abolished by NADPH oxidase inhibitors, but not by other types of inhibitors (Figure 5B). These results suggest that increased levels of fatty acid in accumulated fat seem to stimulate ROS production in adipose cells through the activation of NADPH oxidase.

Effect of ROS on the expression levels of various genes in adipocytes. Next, we examined the effect of ROS in 3T3-L1 adipocytes. Fully differentiated 3T3-L1 adipocytes were exposed to ROS either by treating the cells with H_2O_2 directly, or by an enzymatic method using xanthine oxidase to generate superoxide. The mRNA expression levels of adiponectin and PPARγ were diminished by incubation with H_2O_2 (Figure 6A) in a dose-dependent manner. In contrast, ROS increased the mRNA expression levels of PAI-1, IL-6, and monocyte chemotactic protein–1 (MCP-1) in 3T3-L1 adipocytes (Figure 6A). These changes were also observed by incubation with xanthine oxidase and hypoxanthine (data not shown). Antioxidant NAC reversed the effects of H_2O_2 on the expression levels of these genes to normal levels (Figure 6B). We also found that H_2O_2 increased the mRNA expression levels of NADPH oxidase subunits and PU.1 (Figure 6C), suggesting that ROS itself might augment the NADPH oxidase pathway. Adiponectin secretion by 3T3-L1 adipocytes was also decreased following incubation with H_2O_2, and NAC abrogated the effect of H_2O_2 (Figure 6D). Using a reporter construct containing adiponectin promoter (40), ROS reduced the transcriptional activity of the adiponectin gene in 3T3-L1 adipocytes, and NAC reversed these effects (Figure 6E). These results indicate that ROS downregulated adiponectin expression at the transcriptional level, suggesting that treatment with antioxidants or inhibitors of ROS production might restore the dysregulation of adipocytokines.

Effect of NADPH oxidase inhibitor on adipocytokine expression and glucose and lipid metabolism in KKAy mice. To test the therapeutic effects of the above experimental observations, we treated KKAy mice with the NADPH oxidase inhibitor apocynin (41), and then

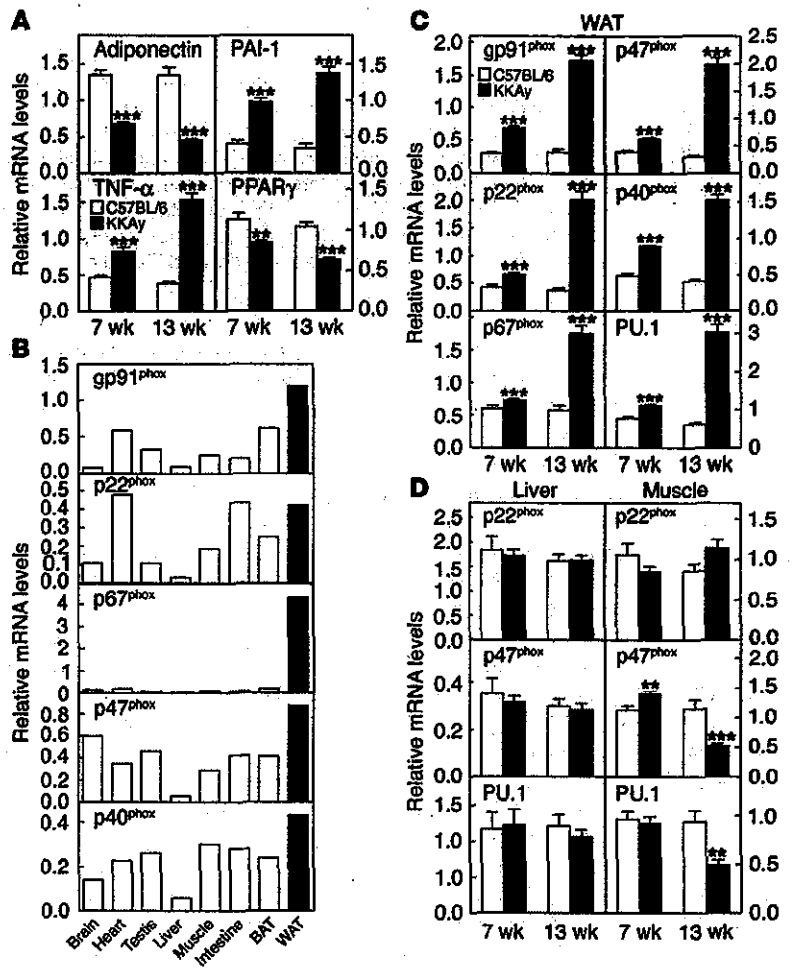

Figure 3
Dysregulated expressions of adipose genes and increased expressions of NADPH oxidase subunits in WAT of obese KKAy mice. (**A**) The mRNA expressions of adiponectin, TNF-α, PAI-1, and PPARγ in WAT of C57BL/6 (white bars) and KKAy (black bars) mice. The mRNA amounts were quantified by real-time PCR. Values are normalized to the level of cyclophilin mRNA, and expressed as mean ± SEM (n = 6–8). (**B**) The mRNA expressions of NADPH oxidase subunits in various mouse tissues. The mRNA amounts were quantified by real-time PCR, using total RNA extracted from 8 tissues of C57BL/6 mice at 12 weeks of age. Values are normalized to the level of 18S ribosomal RNA. (**C** and **D**) The mRNA expressions of NADPH oxidase subunits and PU.1 in WAT (**C**), liver (**D**, left) and skeletal muscle (**D**, right) of C57BL/6 (white bars) and KKAy (black bars) mice at 7 and 13 weeks of age. Values are normalized to the level of cyclophilin mRNA, and expressed as mean ± SEM (n = 6–8). $^{**}P < 0.01$ and $^{***}P < 0.001$ compared with C57BL/6 mice. BAT, brown adipose tissue.

we examined the effects on adipocytokine expression and obesity-associated metabolic disorders. Apocynin is a well-characterized inhibitor of NADPH oxidase activity and is known to impede the assembly of the $p47^{phox}$ subunit with the membrane complex (42). Apocynin is also effective at inhibiting ROS production in various cells in vivo (43, 44). Six-week treatment with apocynin did not affect body weight (Figure 7A) or food intake (data not shown) in control or KKAy mice. Lipid peroxidation and H_2O_2 production in WAT were significantly lower in apocynin-treated KKAy mice than controls (Figure 7, B and C), indicating that NADPH oxidase inhibition reduced oxidative stress in WAT. Similar to the results shown in Figure 2, lipid peroxidation was not altered in the liver and skeletal muscle of KKAy mice, compared to control mice, and it was not affected by apocynin treatment (Supplemental Figure 2). Apocynin treatment increased the mRNA expression of adiponectin in WAT of KKAy mice (Figure 7D), and such an increase was associated with a rise in plasma adiponectin concentration (Figure 7E). Apocynin also decreased the mRNA expression of TNF-α in WAT of KKAy mice (Figure 7D). Apocynin treatment significantly reduced plasma glucose and insulin in KKAy mice but not in C57BL/6 mice (Figure 7F). Plasma triglyceride (TG) levels were also lower in apocynin-treated KKAy mice (Figure 7F). Furthermore, apocynin treatment significantly reduced hepatic TG content in KKAy mice (Figure 7G), suggesting that apocynin could ameliorate hepatic steatosis in KKAy mice. These results showed that inhibition of NADPH oxidase in KKAy mice significantly decreased ROS production by WAT, attenuated the dysregulated production of adipocytokines, and improved the obesity-associated disorders in glucose and lipid metabolism.

Discussion

Obesity is closely associated with metabolic syndrome (1–3). Recent studies have shown that the dysregulated production of "offensive" adipocytokines, such as PAI-1 (10), TNF-α (11, 12), IL-6 (45), MCP-1 (46), and angiotensinogen (47), and of "defensive" adipocytokines, such as adiponectin (18–20) and leptin (15–17), is critically involved in the pathogenesis of metabolic syndrome. However, the mechanisms by which fat accumulation leads to abnormal expression of adipocytokines and development of metabolic syndrome have not been fully elucidated.

In the present study, we have demonstrated that, in nondiabetic human subjects, fat accumulation closely correlated with the markers of systemic oxidative stress. These data are in good agreement with recent studies suggesting that systemic oxidative stress correlates with BMI (48, 49). In addition, we demonstrated that plasma adiponectin levels correlated inversely with systemic oxidative stress. We then reproduced the results of our human studies in several mouse models of obesity, including KKAy, *db/db*, and DIO mice. The

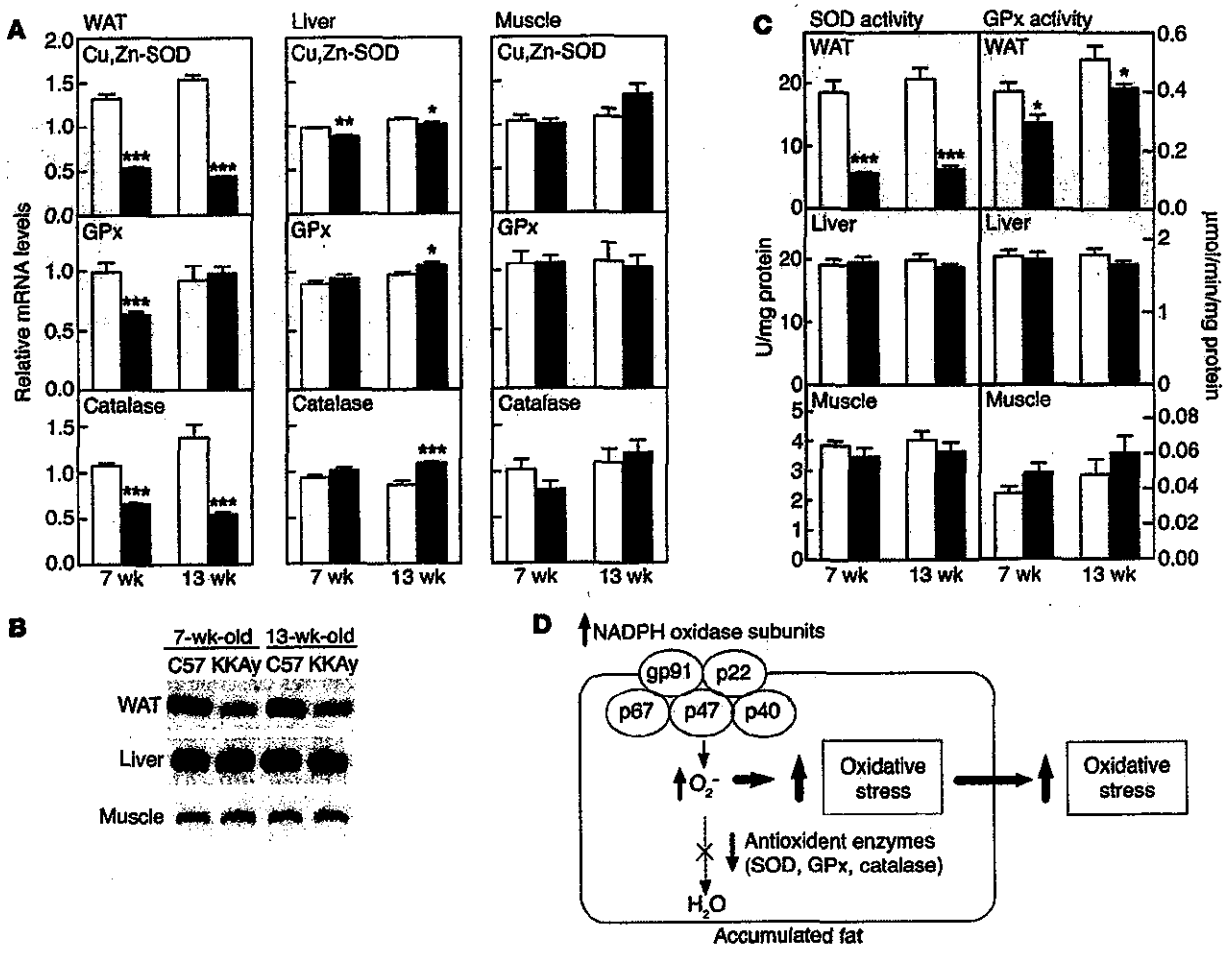

Figure 4
Decreased mRNA expressions and activities of antioxidant enzymes in WAT of obese KKAy mice. (**A**) The mRNA expressions of Cu,Zn-SOD, Gpx, and catalase in WAT, liver, and skeletal muscle of C57BL/6 (white bars) and KKAy (black and gray bars) mice at 7 and 13 weeks of age. Values are normalized to the level of cyclophilin mRNA, and expressed as mean ± SEM (n = 6–8). (**B**) Immunoblot analysis of the amount of Cu,Zn-SOD protein in WAT, liver, and skeletal muscle of C57BL/6 and KKAy mice at 7 and 13 weeks of age. (**C**) Total SOD activities (left) and GPx activities (right) in WAT, liver, and skeletal muscle of C57BL/6 (white bars) and KKAy (black and gray bars) mice at 7 and 13 weeks of age. Values are expressed as mean ± SEM (n = 6–8). (**D**) Model illustrating increased production of oxidative stress in accumulated fat. $^*P < 0.05$, $^{**}P < 0.01$, and $^{***}P < 0.001$ compared with C57BL/6 mice.

main finding of the present study is that oxidative stress in accumulated fat mediates the obesity-associated development of metabolic syndrome by the following potential mechanisms: (a) increased oxidative stress in accumulated fat leads to dysregulated production of adipocytokines, and (b) the selective increase in ROS production in accumulated fat leads to elevation of systemic oxidative stress.

Plasma adiponectin levels correlated inversely with the markers of systemic oxidative stress in nondiabetic human subjects. In cultured adipocytes, addition of oxidative stress suppressed mRNA expression and secretion of adiponectin, and it also increased PAI-1, IL-6, and MCP-1 mRNA expression. Furthermore, treatment with the NADPH oxidase inhibitor apocynin reduced oxidative stress in WAT and increased plasma adiponectin levels in KKAy mice. These results indicate that a local increase in oxidative stress in accumulated fat causes dysregulated production of adipocytokines. Recently, we reported that PPARγ positively regulates the transcription of the adiponectin gene via PPARγ-responsive element in the promoter (40). We showed that oxidative stress suppressed PPARγ mRNA expression in 3T3-L1 adipocytes. It was also shown that nuclear translocation of PPARγ was inhibited by nitration associated with oxidative stress (50). Therefore, downregulation of adiponectin expression may be partially attributed to the decreased gene expression and smaller amount of nuclear PPARγ under conditions of oxidative stress.

In the present study, H_2O_2 production was increased only in adipose tissue of obese mice, but not in other tissues examined, including the liver, skeletal muscle, and aorta. These results suggest that adipose tissue is the major source of the elevated plasma ROS. Oxidative stress is known to impair both insulin secretion by pancreatic β cells (32) and glucose transport in muscle (30) and adipose tissue (31). Increased oxidative stress in vascular walls is involved in the pathogenesis of hypertension (33) and atherosclerosis (34). Oxidative stress also underlies the pathophysiology of hepatic steatosis (51). Thus, oxidative stress locally produced in each of the above

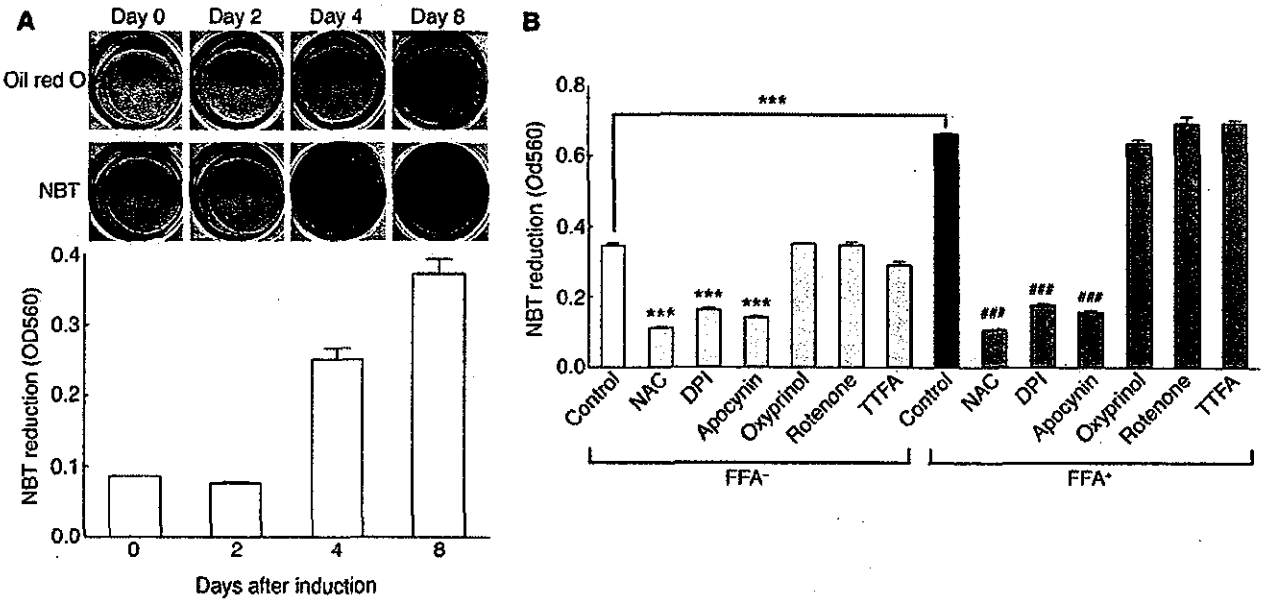

Figure 5

Production of ROS in 3T3-L1 adipocytes. (**A**) ROS production during differentiation of 3T3-L1 cells into adipocytes. ROS production was measured by NBT reduction. Oil red O staining (top) and NBT treatment (middle) of the cells. Dark-blue formazan was dissolved and the absorbance was determined at 560 nm (bottom). (**B**) Effect of linoleate and inhibitors of ROS production in fully differentiated 3T3-L1 adipocytes. 3T3-L1 adipocytes were incubated with (FFA^+) or without (FFA^-) 200 μM linoleate for 24 hours. In the final hour of incubation, 10 mM NAC, 10 μM DPI, 200 μM apocynin, 100 μM oxypurinol, 100 μM rotenone, or 100 μM thenoyltrifluoroacetone (TTFA) was added, and ROS production was measured by NBT reduction. Values are expressed as mean ± SEM ($n = 3$). $^{***}P < 0.001$ compared with cells without linoleate or inhibitors. $^{\#\#\#}P < 0.001$ compared with cells treated with 200 μM linoleate.

tissues seems to be involved in the pathogenesis of these diseases. Our results suggest that increased ROS secretion into peripheral blood from accumulated fat in obesity is also involved in induction of insulin resistance in skeletal muscle and adipose tissue, impaired insulin secretion by β cells, and pathogenesis of various vascular diseases such as atherosclerosis and hypertension.

Why is oxidative stress increased only in accumulated fat? We found that in WAT but not other tissues of obese mice, the mRNA expression levels of NADPH oxidase subunits increased, and mRNA expression levels and activities of antioxidant enzymes decreased. We also found a high level of mRNA expression of the transcription factor PU.1, which upregulates the transcription of the NADPH oxidase gene (37) in adipose tissue of obese mice. Recently, Weisberg et al. (52) and Xu et al. (53) reported that macrophages infiltrated the obese adipose tissues and were an important source of inflammatory cytokines. Since macrophages are also known to produce ROS, it is possible that infiltrated macrophages are involved in augmented NADPH oxidase and elevated ROS production in the obese adipose tissue. In this regard, a family of $gp91^{phox}$ homologs, termed NOX (NADPH oxidase) proteins, has been reported to be expressed in nonphagocytic cells, not in macrophages (54, 55). Recent studies of adipocytes found that NOX4, a member of the NOX family, plays a role in the generation of H_2O_2 (56). The expression of NOX4 was not detected in macrophages (57, 58). In contrast, we found high expression levels of NOX4 in WAT, as well as $gp91^{phox}$, and mRNA expression of NOX4 was significantly increased in WAT of obese mice (Supplemental Figure 3, A and B). These results suggest that adipose NADPH oxidase is elevated and contributes to ROS production in accumulated fat.

We demonstrated that ROS production was increased in 3T3-L1 adipocytes, in parallel with fat accumulation and by incubation with linoleic acid, in a NADPH oxidase–dependent manner. These results suggest that in accumulated fat, elevated levels of fatty acids activate NADPH oxidase and induce ROS production. We also demonstrated that ROS itself augmented mRNA expressions of NADPH oxidase subunits, including NOX4 (Supplemental Figure 3C) and PU.1 in adipocytes. Therefore, in accumulated fat of obesity, elevated ROS appear to upregulate mRNA expression of NADPH oxidase, establishing a vicious cycle that augments oxidative stress in WAT and blood. We found that ROS increased the expression of MCP-1, a chemoattractant for monocytes and macrophages, in adipocytes. Byproducts of lipid peroxidation by ROS, such as *trans*-4-hydroxy-2-nonenal and malondialdehyde, are themselves potent chemoattractants (59). Hence, it is possible that increased ROS production and MCP-1 secretion from accumulated fat should cause infiltration of macrophages and inflammation in adipose tissue of obesity.

Importantly, our in vivo study revealed that treatment with the NADPH oxidase inhibitor apocynin reduced ROS production in adipose tissue of KKAy mice. It also improved hyperinsulinemia, hyperglycemia, hypertriglyceridemia, and hepatic steatosis. Increased expression of adiponectin and decreased expression of TNF-α were observed in WAT of apocynin-treated KKAy mice, demonstrating that reduction of oxidative stress in accumulated fat could improve the dysregulation of adipocytokines in vivo. Our results demonstrate that treatment with NADPH oxidase inhibitor is effective in ameliorating the development of obesity-associated metabolic syndrome.

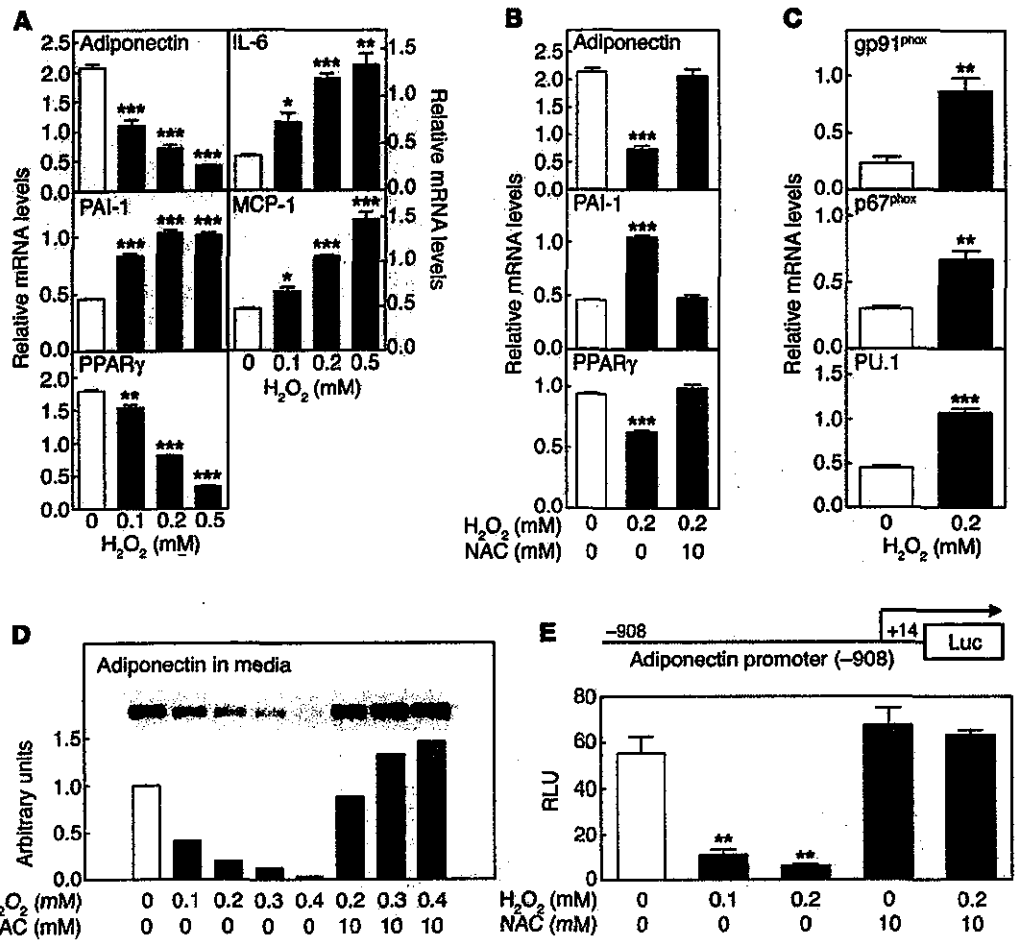

Figure 6

Effects of ROS on gene expressions in 3T3-L1 adipocytes. (**A** and **B**) The mRNA expression levels of adiponectin, PAI-1, PPARγ, IL-6, and MCP-1 in 3T3-L1 adipocytes exposed to ROS, with or without antioxidant NAC. Fully differentiated 3T3-L1 adipocytes were exposed to ROS by incubation with H_2O_2. Values are normalized to the level of cyclophilin mRNA and expressed as mean ± SEM (n = 3). (**C**) The mRNA expression levels of NADPH oxidase subunits and PU.1 in 3T3-L1 adipocytes exposed to ROS. Values are normalized to the level of cyclophilin mRNA. (**D**) Effects of H_2O_2 and NAC on adiponectin secretion from 3T3-L1 adipocytes. Adiponectin levels in the media were determined by Western blotting (inset) and the values were quantified using a densitometer. (**E**) Effects of ROS and NAC on the transcriptional activity of adiponectin promoter in 3T3-L1 adipocytes. RLU, relative luciferase units. Values are expressed as mean ± SEM (n = 3). $^*P < 0.05$, $^{**}P < 0.01$, and $^{***}P < 0.001$ compared with control.

It has been reported that prolonged exposure of 3T3-L1 adipocytes to ROS results in impairments of insulin-induced activation of PI3-kinase and Akt, insulin-stimulated lipogenesis, glucose uptake, and GLUT4 translocation to the plasma membrane (31, 60). Thus, NADPH oxidase inhibitors might improve insulin sensitivity via suppression of these effects induced by chronic exposure to ROS. Our current results are consistent with several previous studies demonstrating that antioxidant treatment improves insulin function in diabetic subjects (61, 62).

Recent studies, on the other hand, have proposed that ROS such as H_2O_2 are produced transiently in response to insulin stimulation and also act as a second messenger for insulin signaling in adipocytes (63, 64). NADPH oxidase is thought to be involved in insulin-induced ROS generation (63, 64). We assume that a transient increase of intracellular ROS is important for the insulin signaling pathway, while excessive and long-term exposure to ROS reduces insulin sensitivity and impairs glucose and lipid metabolism.

In the present study, we observed stimulation of ROS production by fatty acids via NADPH oxidase activation. In addition, we also found that ROS suppressed the mRNA expressions of lipogenic genes, such as fatty acid synthase and sterol regulatory element binding protein-1c, in 3T3-L1 adipocytes (data not shown). These results suggest that increased ROS production caused by fat accumulation may prevent further lipid storage, but may simultaneously cause dysregulated expression of adipocytokines and insulin resistance. Conceivably, inhibition of NADPH oxidase should improve the dysregulation of adipocytokines and insulin sensitivity via restoration of normal ROS production in obese adipocytes.

Figure 8 illustrates our working hypothesis regarding the role of ROS in metabolic syndrome. Increased oxidative stress in accumulated fat, via increased NADPH oxidase and decreased antioxidant enzymes, causes dysregulated production of adipocytokines, locally. Increased ROS production from accumulated fat also leads to increased oxidative stress in blood, hazardously affecting other organs including the liver, skeletal muscle, and aorta. We propose that increased oxidative stress in accumulated fat is an early instigator and one of the important underlying causes of obesity-associated metabolic syndrome, hence, the redox state in adipose tissue is a potentially useful target in new therapies against obesity-associated metabolic syndrome, as we demonstrated in the mouse in vivo study.

Methods

Subjects. Plasma and urinary samples were obtained after overnight fasting from 140 subjects (69 men and 71 women; mean age 56 ± 13 SD) who visited the University hospital for a healthy checkup. Patients with a history of diabetes, cardiovascular or cerebrovascular disease, hepatic or renal disease,

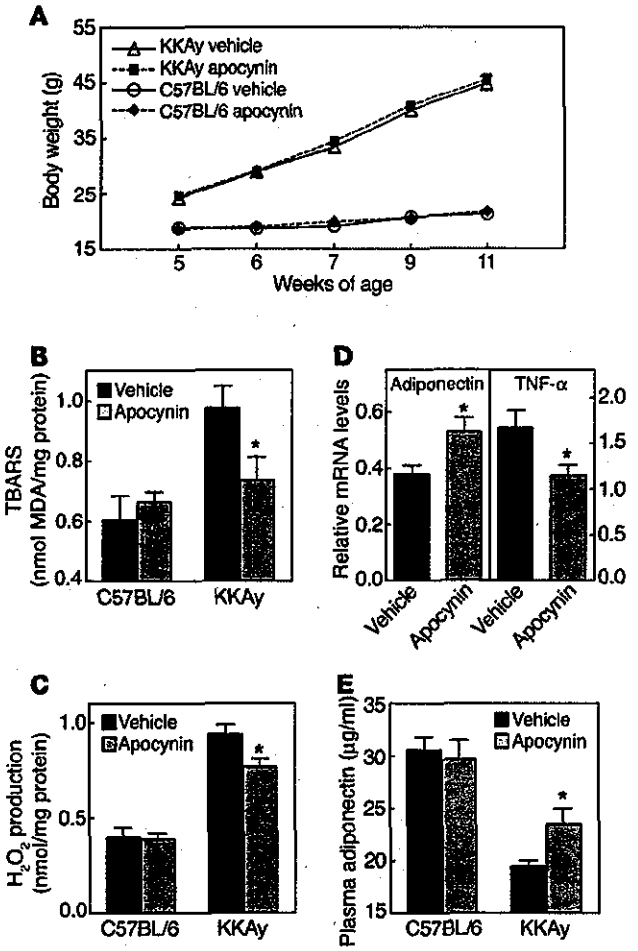

Figure 7
In vivo effects of an NADPH oxidase inhibitor, apocynin, on adipocytokine expression, and glucose and lipid metabolism in KKAy mice. **(A)** Body weight of C57BL/6 and KKAy mice, treated with or without apocynin for 6 weeks. **(B)** Lipid peroxidation in WAT, and **(C)** release of H_2O_2 from WAT of C57BL/6 and KKAy mice, treated with or without apocynin for 6 weeks. **(D)** The mRNA expression levels of adiponectin and TNF-α in WAT of KKAy mice. Values are normalized to the level of cyclophilin mRNA. **(E)** Plasma adiponectin concentrations in C57BL/6 and KKAy mice. **(F)** Plasma glucose, insulin, and TG concentrations in C57BL/6 and KKAy mice. **(G)** Liver TG content in C57BL/6 and KKAy mice. Values are expressed as mean ± SEM (n = 8). *P < 0.05 and **P < 0.01 compared with vehicle-treated group.

tobacco abuse, or those on hormone replacement therapy were excluded. The study protocols complied with the Guidelines of the Ethical Committees of Osaka University and University of the Ryukyus. Informed consent was obtained from all subjects. Samples were stored at -80°C until use.

Animals. All animals were purchased from Clea Japan and housed in a room under controlled temperature (23 ± 1°C) and humidity (45–65%) and had free access to water and chow (Oriental Yeast Co.). All animal experiments were conducted in accordance with the aforementioned institutional guidelines for the care and use of laboratory animals. Female C57BL/6J and KKAy mice at 7 or 13 weeks of age were anesthetized using pentobarbital sodium, blood was collected, and parametrial WAT, liver tissue, and gastrocnemius muscle were dissected out and frozen in liquid nitrogen. Samples were stored at -80°C until use. For DIO studies, male C57BL/6J mice were divided at random into 2 groups at 10 weeks of age. The first group was fed a high-fat diet containing 30% fat by weight (AIN93G) while the second group was fed normal chow containing 5.9% fat by weight (CRF-1; Oriental Yeast Co.) for 9 weeks. After an overnight fast, mice were anesthetized, and blood and tissue samples were obtained as described above.

Biochemical measurements. Urinary 8-epi-PGF2α was determined using an enzyme immunoassay kit (Assay Designs Inc.). Plasma levels of glucose and TG were measured using the Glucose-test and TG E-test, respectively, from Wako Pure Chemical Industries. Plasma adiponeccin levels were determined using the Adiponectin ELISA kit (Otsuka). Plasma insulin levels were assessed using an insulin ELISA kit (Shibayagi).

Lipid peroxidation and hydrogen peroxide concentration. Tissue samples were homogenized in a buffer solution containing 50 mM Tris-HCl (pH 7.4) and 1.15% KCl, and then centrifuged. The supernatant was used for the assay. The levels of lipid peroxidation in plasma and tissue homogenate were measured as TBARS using the LPO-test (Wako Pure Chemical Industries). Hydrogen peroxide concentration in plasma was measured using an Amplex Red hydrogen peroxide assay kit (Invitrogen Corp.).

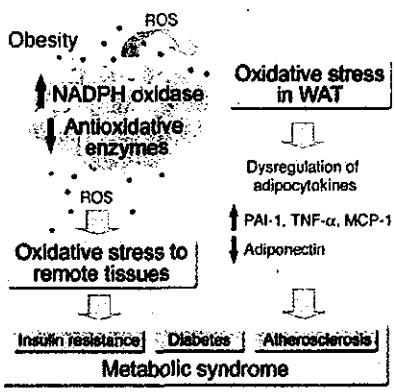

Figure 8
A working model illustrating how increased ROS production in accumulated fat contributes to metabolic syndrome.

H_2O_2 production. Female C57BL/6J and KKAy mice at 7 weeks of age were anesthetized. Parametrial WAT and gastrocnemius muscle were dissected out and placed in Krebs-Ringer phosphate buffer containing (in mM) 145 NaCl, 5.7 sodium phosphate, 4.86 KCl, 0.54 $CaCl_2$, 1.22 $MgSO_4$, and 5.5 glucose (pH 7.4). The aorta was carefully removed, cleaned of excess fat and adventitia, and placed in Krebs-Ringer phosphate buffer. WAT, muscle, and aorta were cut into 2-mm square pieces and incubated at 37°C for 90 minutes. H_2O_2 released from the tissue was detected using the Amplex Red hydrogen peroxide assay kit (Invitrogen Corp.).

Quantitative RT-PCR. Total RNA from WAT, liver, and skeletal muscle were prepared with an RNA STAT-60 kit (Tel-Test "B" Inc.). The cDNA was synthesized using the ThermoScript RT-PCR System (Invitrogen Corp.). Real-time PCR was performed on a LightCycler using the FastStart DNA Master SYBR Green I (Roche Diagnostics) according to the protocol provided by the manufacturer. Sequences of primers used for real-time PCR were as follows: Adiponectin, 5′-GATGGCAGAGATGGCACTCC-3′ and 5′-CTTGCCAGTGCTGCCGTCAT-3′; TNF-α, 5′-GCCACCACGCTCTTCTG-3′ and 5′-GGTGTGGGTGAGGAGCA-3′; PAI-1, 5′-TCAGCCCTTGCTTGCCTCAT-3′ and 5′-GCATAGCCAGCACCGAGGA-3′; IL-6, 5′-ACAACCACGGCCTTCCCTACTT-3′ and 5′-CACGATTTCCCAGAGAACATGTG-3′; MCP-1, 5′-CCACTCACCTGCTGCTACTCAT-3′ and 5′-TGGTGATCCTCTTGTAGCTCTCC-3′; PPARγ, 5′-CCAGAGTCTGCTGATCTGCG-3′ and 5′-GCCACCTCTTTGCTCTGCTC-3′; $gp91^{phox}$, 5′-TTGGGTCAGCACTGGCTCTG-3′ and 5′-TGGCGGTGTGCAGTGCTATC-3′; $p22^{phox}$, 5′-GTCCACCATGGAGCGATGTG-3′ and 5′-CAATGGCCAAGCAGACGGTC-3′; $p67^{phox}$, 5′-CTGGCTGAGGCCATCAGACT-3′ and 5′-AGGCCACTGCAGAGTGCTTG-3′; $p47^{phox}$, 5′-GATGTTCCCCATTGAGGCCG-3′ and 5′-GTTTCAGGTCATCAGGCCGC-3′; $p40^{phox}$, 5′-GCCGCTATCGCCAGTTCTAC-3′ and 5′-GCAGGCTCAGGAGGTTCTTC-3′; Cu,Zn-SOD, 5′-CAGCATGGGTTCCACGTCCA-3′ and 5′-CACATTGGCCACACCGTCCT-3′; glutathione peroxidase, 5′-GGGCAAGGTGCTGCTCATTG-3′ and 5′-AGAGCGGGTGAGCCTTCTCA-3′; catalase, 5′-CCAGCGACCAGATGAAGCAG-3′ and 5′-CCACTCTCTCAGGAATCCGC-3′; cyclophilin, 5′-CAGACGCCACTGTCGCTTT-3′ and 5′-TGTCTTTGGAACTTTGTCTGCAA-3′; 18S ribosomal RNA, 5′-CGGCTACCACATCCAAGGAA-3′ and 5′-GCTGGAATTACCGCGGCT-3′.

Antioxidant enzyme activity. Tissue homogenates were prepared as above. SOD activity was measured using the BIOXYTECH SOD-525 kit (Oxis International). GPx activity was measured using the method described previously (65).

Western blot analysis. Tissue homogenates (20 μg protein) were subjected to SDS-PAGE, and immunoblotting was performed with anti–Cu,Zn-SOD polyclonal antibody (Upstate Biotechnology).

ROS production in 3T3-L1 adipocytes. 3T3-L1 preadipocytes were grown to confluence and induced to differentiate into adipocytes, as described (40). ROS production was detected by nitroblue tetrazolium (NBT) assay (35). NBT is reduced by ROS to a dark-blue, insoluble form of NBT called formazan. At days 0, 2, 4, and 8 after induction, 3T3-L1 cells were incubated for 90 minutes in PBS containing 0.2% NBT. Formazan was dissolved in 50% acetic acid, and the absorbance was determined at 560 nm. Fully differentiated 3T3-L1 adipocytes were incubated with or without 200-μM linoleic acid for 24 hours. Various inhibitors were added in the last hour of incubation, and the cells were incubated for 90 minutes in PBS containing 0.2% NBT with or without inhibitors. NBT, DPI, NAC, oxypurinol, rotenone, and thenoyltrifluoroacetone were purchased from Sigma-Aldrich. Apocynin was purchased from Calbiochem.

Effect of ROS on expression of genes in 3T3-L1 adipocytes. At day 8 after induction, fully differentiated 3T3-L1 adipocytes were exposed to ROS by incubation with fresh medium containing xanthine oxidase plus hypoxanthine or H_2O_2 for 24 hours, with or without 10-mM NAC. Cells were harvested, total RNAs were extracted, and the mRNA amounts were quantified by real-time PCR, as described above. The levels of adiponectin in media were determined by Western blotting (40). Transfection experiments were performed as described previously (40). At day 4 after induction, 3T3-L1 cells in 12-well plates were transfected with 1 μg of the reporter construct containing the fragment corresponding to base pairs −908 to +14 of the human adiponectin promoter linked to a luciferase reporter gene, along with 0.5 μg of pCMX-β-gal (internal standard). Four hours later, cells were exposed to ROS for 20 hours, with or without 10 mM NAC. Luciferase activities were assayed using Luciferase Assay System (Promega Corp.). Values were normalized by an internal β-galactosidase control and expressed as the relative luciferase activity.

NADPH oxidase inhibitor treatment. At 5 weeks of age, female C57BL/6J and KKAy mice were treated for 6 weeks with 5 mM apocynin added to the drinking water. At 11 weeks of age, the mice, fed ad libitum, were anesthetized using pentobarbital sodium, blood was collected, and parametrial WAT, liver, and skeletal muscle were dissected out for physiologic analyses. The liver TG contents were measured as described previously (66).

Statistical analysis. In the human study, linear regression analysis was used to evaluate the relationship between 2 variables. All data are presented as mean ± SEM and were analyzed using unpaired Student's *t* tests. *P* values less than 0.05 were considered statistically significant.

Acknowledgments

We are grateful to Hitoshi Nishizawa and Atsunori Fukuhara for the critical reading of the manuscript, Yoshihiro Tochino for excellent technical assistance, and Sumio Kiyoto for the helpful comments. We thank all members of the Shimomura laboratory for the helpful discussion and comments. This study was supported in part by Suzuken Memorial Foundation, the Tokyo Biochemical Research Foundation, Takeda Medical Research Foundation, Uehara Memorial Foundation, Takeda Science Foundation, Novartis Foundation of Japan for the Promotion of Science, the Cell Science Research Foundation, the Mochida Memorial Foundation for Medical and Pharmaceutical Research, a grant-in-aid from the Japan Medical Association, the Naito Foundation, a grant from the Japan Heart Foundation Research, Kato Memorial Bioscience Foundation, Japan Research Foundation for Clinical Pharmacology, the 21st century COE program, the Japan Society for the Promotion of Science, grants from the Ministry of Health, Labor and Welfare of Japan, and grants from the Ministry of Education, Culture, Sports, Science and Technology of Japan.

Received for publication March 17, 2004, and accepted in revised form October 19, 2004.

Address correspondence to: Iichiro Shimomura, Department of Internal Medicine and Molecular Science, Graduate School of Medicine, Osaka University, 2-2 Yamadaoka, Suita, Osaka 565-0871, Japan. Phone: 81-6-6879-3730; Fax: 81-6-6879-3739; E-mail: ichi@imed2.med.osaka-u.ac.jp. Or to: Morihiro Matsuda, Department of Medicine and Pathophysiology, Graduate School of Medicine, Department of Organismal Biosystems, Graduate School of Frontier Biosciences, Osaka University, 2-2 Yamadaoka, Suita, Osaka 565-0871, Japan. Phone: 81-6-6879-3273; Fax: 81-6-6879-3279; E-mail: mmatsuda@fbs.osaka-u.ac.jp.

Makoto Makishima's present address is: Department of Biochemistry, Nihon University School of Medicine, Tokyo, Japan.

1. Isomaa, B., et al. 2001. Cardiovascular morbidity and mortality associated with the metabolic syndrome. *Diabetes Care.* **24**:683–689.
2. Ford, E.S., Giles, W.H., and Dietz, W.H. 2002. Prevalence of the metabolic syndrome among US adults: findings from the Third National Health and Nutrition Examination Survey. *JAMA.* **287**:356–359.
3. Grundy, S.M., et al. 2004. Definition of metabolic syndrome: Report of the National Heart, Lung, and Blood Institute/American Heart Association conference on scientific issues related to definition. *Circulation.* **109**:433–438.
4. Montague, C.T., and O'Rahilly, S. 2000. The perils of portliness: causes and consequences of visceral adiposity. *Diabetes.* **49**:883–888.
5. Matsuzawa, Y., Funahashi, T., and Nakamura, T. 1999. Molecular mechanism of metabolic syndrome X: Contribution of adipocytokines adipocyte-derived bioactive substances. *Ann. N. Y. Acad. Sci.* **892**:146–154.
6. Spiegelman, B.M., and Flier, J.S. 2001. Obesity and the regulation of energy balance. *Cell.* **104**:531–543.
7. Kahn, B.B., and Flier, J.S. 2000. Obesity and insulin resistance. *J. Clin. Invest.* **106**:473–481.
8. Friedman, J.M. 2000. Obesity in the new millennium. *Nature.* **404**:632–634.
9. Saltiel, A.R., and Kahn, C.R. 2001. Insulin signaling and the regulation of glucose and lipid metabolism. *Nature.* **414**:799–806.
10. Shimomura, I., et al. 1996. Enhanced expression of PAI-1 in visceral fat: possible contributor to vascular disease in obesity. *Nat. Med.* **2**:800–803.
11. Hotamisligil, G.S., Shargill, N.S., and Spiegelman, B.M. 1993. Adipose expression of tumor necrosis factor-α: direct role in obesity-linked insulin resistance. *Science.* **259**:87–91.
12. Uysal, K.T., Wiesbrock, S.M., Marino, M.W., and Hotamisligil, G.S. 1997. Protection from obesity-induced insulin resistance in mice lacking TNF-alpha function. *Nature.* **389**:610–614.
13. Steppan, C.M., et al. 2001. The hormone resistin links obesity to diabetes. *Nature.* **409**:307–312.
14. Banerjee, R.R., et al. 2004. Regulation of fasted blood glucose by resistin. *Science.* **303**:1195–1198.
15. Friedman, J.M., and Halaas, J.L. 1998. Leptin and the regulation of body weight in mammals. *Nature.* **395**:763–770.
16. Farooqi, I.S., et al. 2001. Partial leptin deficiency and human adiposity. *Nature.* **414**:34–35.
17. Unger, R.H. 2003. The physiology of cellular liporegulation. *Annu. Rev. Physiol.* **65**:333–347.
18. Berg, A.H., Combs, T.P., and Scherer, P.E. 2002. ACRP30/adiponectin: An adipokine regulating glucose and lipid metabolism. *Trends Endocrinol. Metab.* **13**:84–89.
19. Tsao, T.S., Lodish, H.F., and Fruebis, J. 2002. ACRP30, a new hormone controlling fat and glucose metabolism. *Eur. J. Pharmacol.* **440**:213–221.
20. Matsuzawa, Y., Funahashi, T., Kihara, S., and Shimomura, I. 2004. Adiponectin and metabolic syndrome. *Arterioscler. Thromb. Vasc. Biol.* **24**:29–33.
21. Arita, Y., et al. 1999. Paradoxical decrease of an adipose-specific protein, adiponectin, in obesity. *Biochem. Biophys. Res. Commun.* **257**:79–83.
22. Fruebis, J., et al. 2001. Proteolytic cleavage product of 30-kDa adipocyte complement-related protein increases fatty acid oxidation in muscle and causes weight loss in mice. *Proc. Natl. Acad. Sci. U. S. A.* **98**:2005–2010.
23. Yamauchi, T., et al. 2001. The fat-derived hormone adiponectin reverses insulin resistance associated with both lipoatrophy and obesity. *Nat. Med.* **7**:941–946.
24. Berg, A.H., Combs, T.P., Du, X., Brownlee, M., and Scherer, P.E. 2001. The adipocyte-secreted protein Acrp30 enhances hepatic insulin action. *Nat. Med.* **7**:947–953.
25. Maeda, N., et al. 2002. Diet-induced insulin resistance in mice lacking adiponectin/ACRP30. *Nat. Med.* **8**:731–737.
26. Okamoto, Y., et al. 2002. Adiponectin reduces atherosclerosis in apolipoprotein E-deficient mice. *Circulation.* **106**:2767–2770.
27. Matsuda, M., et al. 2002. Role of adiponectin in preventing vascular stenosis. The missing link of adipovascular axis. *J. Biol. Chem.* **277**:37487–37491.
28. Yamauchi, T., et al. 2003. Globular adiponectin protected ob/ob mice from diabetes and apoE-deficient mice from atherosclerosis. *J. Biol. Chem.* **278**:2461–2468.
29. Brownlee, M. 2001. Biochemistry and molecular cell biology of diabetic complications. *Nature.* **414**:813–820.
30. Maddux, B.A., et al. 2001. Protection against oxidative stress-induced insulin resistance in rat L6 muscle cells by micromolar concentrations of α-lipoic acid. *Diabetes.* **50**:404–410.
31. Rudich, A., et al. 1998. Prolonged oxidative stress impairs insulin-induced GLUT4 translocation in 3T3-L1 adipocytes. *Diabetes.* **47**:1562–1569.
32. Matsuoka, T., et al. 1997. Glycation-dependent, reactive oxygen species-mediated suppression of the insulin gene promoter activity in HIT cells. *J. Clin. Invest.* **99**:144–150.
33. Nakazono, K., et al. 1991. Does superoxide underlie the pathogenesis of hypertension? *Proc. Natl. Acad. Sci. U. S. A.* **88**:10045–10048.
34. Ohara, Y., Peterson, T.E., and Harrison, D.G. 1993. Hypercholesterolemia increases endothelial superoxide anion production. *J. Clin. Invest.* **91**:2546–2551.
35. Oliveira, H.R., et al. 2003. Pancreatic β-cells express phagocyte-like NAD(P)H oxidase. *Diabetes.* **52**:1457–1463.
36. Griendling, K.K., Sorescu, D., and Ushio-Fukai, M. 2000. NAD(P)H oxidase: role in cardiovascular biology and disease. *Circ. Res.* **86**:494–501.
37. Li, S., Valente, A.J., Zhao, S., and Clark, R.A. 1997. PU.1 is essential for p47phox promoter activity in myeloid cells. *J. Biol. Chem.* **272**:17802–17809.
38. Nishikawa, T., et al. 2000. Normalizing mitochondrial superoxide production blocks three pathways of hyperglycaemic damage. *Nature.* **404**:787–790.
39. Inoguchi, T., et al. 2000. High glucose level and free fatty acid stimulate reactive oxygen species production through protein kinase C-dependent activation of NAD(P)H oxidase in cultured vascular cells. *Diabetes.* **49**:1939–1945.
40. Iwaki, M., et al. 2003. Induction of adiponectin, a fat-derived antidiabetic and antiatherogenic factor, by nuclear receptors. *Diabetes.* **52**:1655–1663.
41. Simons, J.M., Hart, B.A., Ip Vai Ching, T.R., Van Dijk, H., and Labadie, R.P. 1990. Metabolic activation of natural phenols into selective oxidative burst agonists by activated human neutrophils. *Free Radic. Biol. Med.* **8**:251–258.
42. Meyer, J.W., et al. 1990. Identification of a function leukocyte-type NADPH oxidase in human endothelial cells: a potential atherogenic source of reactive oxygen species. *Endothelium.* **7**:11–22.
43. Beswick, R.A., Dorrance, A.M., Leite, R., and Webb, R.C. 2001. NADH/NADPH oxidase and enhanced superoxide production in the mineralocorticoid hypertensive rat. *Hypertension.* **38**:1107–1111.
44. Cotter, M.A., and Cameron, N.E. 2003. Effect of the NAD(P)H oxidase inhibitor, apocynin, on peripheral nerve perfusion and function in diabetic rats. *Life Sci.* **73**:1813–1824.
45. Fried, S.K., Bunkin, D.A., and Greenberg, A.S. 1998. Omental and subcutaneous adipose tissues of obese subjects release interleukin-6: depot difference and regulation by glucocorticoid. *J. Clin. Endocrinol. Metab.* **83**:847–850.
46. Sartipy, P., and Loskutoff, D.J. 2003. Monocyte chemoattractant protein 1 in obesity and insulin resistance. *Proc. Natl. Acad. Sci. U. S. A.* **100**:7265–7270.
47. Hainault, I., et al. 2002. Adipose tissue-specific increase in angiotensinogen expression and secretion in the obese (fa/fa) zucker rat. *Am. J. Physiol. Endocrinol. Metab.* **282**:E59–E66.
48. Keaney, J.F., Jr., et al. 2003. Obesity and systemic oxidative stress: clinical correlates of oxidative stress in the Framingham Study. *Arterioscler. Thromb. Vasc. Biol.* **23**:434–439.
49. Olusi, S.O. 2002. Obesity is an independent risk factor for plasma lipid peroxidation and depletion of erythrocyte cytoprotective enzymes in humans. *Int. J. Obes. Relat. Metab. Disord.* **26**:1159–1164.
50. Shibuya, A., et al. 2002. Nitration of PPARγ inhibits ligand-dependent translocation into the nucleus in a macrophage-like cell line, RAW 264. *FEBS Lett.* **525**:43–47.
51. Roskams, T., et al. 2003. Oxidative stress and oval cell accumulation in mice and humans with alcoholic and nonalcoholic fatty liver disease. *Am. J. Pathol.* **163**:1301–1311.
52. Weisberg, S.P., et al. 2003. Obesity is associated with macrophage accumulation in adipose tissue. *J. Clin. Invest.* **112**:1796–1808. doi:10.1172/JCI200319246.
53. Xu, H., et al. 2003. Chronic inflammation in fat plays a crucial role in the development of obesity-related insulin resistance. *J. Clin. Invest.* **112**:1821–1830. doi:10.1172/JCI200319451.
54. Shiose, A., et al. 2001. A novel superoxide-producing NAD(P)H oxidase in kidney. *J. Biol. Chem.* **276**:1417–1423.
55. Suh, Y.A., et al. 1999. Cell transformation by the superoxide-generating oxidase Mox1. *Nature.* **401**:79–82.
56. Mahadev, K., et al. 2004. The NAD(P)H oxidase homolog Nox4 modulates insulin-stimulated generation of H_2O_2 and plays an integral role in insulin signal transduction. *Mol. Cell. Biol.* **24**:1844–1854.
57. Yang, S., Zhang, Y., Ries, W., and Key, L. 2004. Expression of Nox4 in osteoclasts. *J. Cell. Biochem.* **92**:238–248.
58. Sorescu, D., et al. 2002. Superoxide production and expression of Nox family proteins in human atherosclerosis. *Circulation.* **105**:1429–1435.
59. Curzio, M., et al. 1987. Possible role of aldehydic lipid peroxidation products as chemoattractants. *Int. J. Tissue React.* **9**:295–306.
60. Tirosh, A., Potashnik, R., Bashan, N., and Rudich, A. 1999. Oxidative stress disrupts insulin-induced cellular redistribution of insulin receptor substrate-1 and phosphatidylinositol 3-kinase in 3T3-L1 adipocytes. *J. Biol. Chem.* **274**:10595–10602.
61. Jacob, S., et al. 1999. Oral administration of RAC-alpha-lipoic acid modulates insulin sensitivity in patients with type-2 diabetes mellitus: a placebo-controlled pilot trial. *Free Radic. Biol. Med.* **27**:309–314.
62. Evans, J.L., Goldfine, I.D., Maddux, B.A., and Grodsky, G.M. 2002. Oxidative stress and stress-activated signaling pathways: A unifying hypothesis of type 2 diabetes. *Endocrine Rev.* **23**:599–622.
63. Krieger-Brauer, H.I., and Kather, H. 1992. Human fat cells possess a plasma membrane-bound H_2O_2-generating system that is activated by insulin via a mechanism bypassing the receptor kinase. *J. Clin. Invest.* **89**:1006–1013.
64. Krieger-Brauer, H.I., and Kather, H. 1995. Antagonistic effects of different members of the fibroblast and platelet-derived growth factor families on adipose conversion and NADPH-dependent H_2O_2 generation in 3T3-L1 cells. *Biochem. J.* **307**:549–556.
65. Takahashi, K. 2000. Glutathione peroxidase: coupled enzyme assay. In *Experimental protocols for reactive oxygen and nitrogen species.* N. Taniguchi and J.M.C. Gutteridge, editors. Oxford University Press. Oxford, United Kingdom. 79–80.
66. Yokode, M., Hammer, R.E., Ishibashi, S., Brown, M.S., and Goldstein, J.L. 1990. Diet-induced hypercholesterolemia in mice: prevention of overexpression of LDL receptors. *Science.* **250**:1273–1275.

THE JOURNAL OF BIOLOGICAL CHEMISTRY
Vol. 279, No. 41, Issue of October 8, pp. 42867–42874, 2004
Printed in U.S.A.

Intectin, a Novel Small Intestine-specific Glycosylphosphatidylinositol-anchored Protein, Accelerates Apoptosis of Intestinal Epithelial Cells*

Received for publication, July 16, 2004
Published, JBC Papers in Press, July 28, 2004, DOI 10.1074/jbc.M408047200

Hidefumi Kitazawa,[a,b,c] Tamao Nishihara,[a,b,d] Tadahiro Nambu,[e] Hitoshi Nishizawa,[a,f] Masanori Iwaki,[a] Atsunori Fukuhara,[a] Toshio Kitamura,[g] Morihiro Matsuda,[a,d,h] and Iichiro Shimomura[a,f,i,j]

From the [a]Department of Medicine and Pathophysiology, Graduate School of Frontier Bioscience, Graduate School of Medicine, Osaka University, 2-2 Yamadaoka, Suita, Osaka 565-0871, the [e]Tsukuba Research Institute, Banyu Pharmaceutical Co., Ltd., Okubo 3, Tsukuba 300-2611, the [f]Department of Internal Medicine and Molecular Science, Graduate School of Medicine, Osaka University, 2-2 Yamadaoka, Suita, Osaka 565-0871, the [g]Department of Hematopoietic Factors, Institute of Medical Science, University of Tokyo, Minato-ku, Tokyo 108-8639, [i]Precursory Research for Embryonic Science and Technology, Japan Science and Technology Agency, 4-1-8 Honcho, Kawaguchi, Saitama 332-0012, and the [d]21st Century Center of Excellence Program, the Japan Society for the Promotion of Science, Tokyo 102-8471, Japan

Intestinal epithelial cells undergo rapid turnover and exfoliation especially at the villus tips. This process is modulated by various nutrients especially fat. Apoptosis is one of the important regulatory mechanisms of this turnover. Therefore, identification of the factors that control epithelial cell apoptosis should help us understand the mechanism of intestinal mucosal turnover. Here, we report the identification of a novel small intestine-specific member of the Ly-6 family, intectin, by signal sequence trap method. Intectin mRNA expression was exclusively identified in the intestine and localized at the villus tips of intestinal mucosa, which is known to undergo apoptosis. Intectin mRNA expression was modulated by nutrition. Intestinal epithelial cells expressing intectin were more sensitive to palmitate-induced apoptosis, compared with control intestinal epithelial cells, and such effect was accompanied by increased activity of caspase-3. Intectin expression also reduced cell-cell adhesion of intestinal epithelial cells.

Intestinal epithelial cells originate from stem cells at the base of the crypt and migrate along the crypt-villus axis toward the intestinal lumen. When intestinal epithelial cells reach the luminal surface at the villus tips, they finally exfoliate into the lumen, and their cell cycle is terminated with a life span of only 3–5 days (1, 2). This constant and rapid turnover of intestinal mucosa is essential for maximal nutrient absorption, adaptation to changes in diet, and repair of mucosal injury (3).

Apoptosis plays an important role in maintaining the physiological integrity of many tissues. In the intestine, apoptosis is a key regulator for the turnover of intestinal mucosa, and apoptotic intestinal epithelial cells have been detected at the villus tips of the small intestine and the colonic luminal surface (4–6). However, the one or more underlying mechanisms of this process have not been elucidated. In this regard, it is important to identify the factors that control intestinal epithelial cell apoptosis to understand the mechanism of intestinal mucosal turnover.

The present study was designed to identify a small intestine-derived protein or secretory protein modulated nutritionally that is involved in the control of intestinal epithelial cell apoptosis. Using the efficient signal sequence trap (SST)[1] method (7), we identified a novel small intestine-specific GPI-anchored protein, intectin, which showed distinct localization at the villus tips of intestinal mucosa and accelerated fatty acid-induced apoptosis of intestinal epithelial cells.

EXPERIMENTAL PROCEDURES

Cloning of Intectin cDNA—Poly(A)$^+$ RNAs were extracted from the small intestinal epithelium of C57BL/6J mice under three feeding conditions; *ad libitum*, 24-h fasting, and 24-h fasting followed by 24-h feeding, and from the small intestinal epithelium of *ad libitum*-fed *db/db* mice. Equal amount of poly(A)$^+$ RNA from each group was pooled and used as the template to synthesize complementary DNA (cDNA). To selectively clone the genes with signal sequence at the N-terminal end of cDNAs, the SST-REX system (signal sequence trap

* This work was supported by The Suzuken Memorial Foundation, The Nakajima Foundation, the Kanae Foundation for Life and Socio-Medical Science, The Tokyo Biochemical Research Foundation, the Takeda Medical Research Foundation, Uehara Memorial Foundation, the Takeda Science Foundation, the Novartis Foundation (Japan) for the Promotion of Science, The Cell Science Research Foundation, The Mochida Memorial Foundation for Medical and Pharmaceutical Research, a Grant-in-Aid from the Japan Medical Association, The Naito Foundation, a grant from the Japan Heart Foundation Research, the Kato Memorial Bioscience Foundation, the Japan Research Foundation for Clinical Pharmacology, a grant from the Ministry of Health, Labor, and Welfare, Japan, and grants from the Ministry of Education, Culture, Sports, Science, and Technology, Japan. The costs of publication of this article were defrayed in part by the payment of page charges. This article must therefore be hereby marked "*advertisement*" in accordance with 18 U.S.C. Section 1734 solely to indicate this fact.

[b] Both authors contributed equally to this work.
[c] Present address: Tsukuba Research Institute, Banyu Pharmaceutical Co., Ltd., Okubo 3, Tsukuba 300-2611, Japan.
[h] To whom correspondence may be addressed: Dept. of Medicine and Pathophysiology, Graduate School of Frontier Bioscience, Graduate School of Medicine, Osaka University, 2-2 Yamadaoka, Suita, Osaka 565-0871, Japan. Tel.: 81-6-6879-3272; Fax: 81-6-6879-3279; E-mail: mmatsuda@fbs.osaka-u.ac.jp.
[j] To whom correspondence may be addressed: Dept. of Internal Medicine and Molecular Science, Graduate School of Medicine, Osaka University, 2-2 Yamadaoka, Suita, Osaka 565-0871, Japan. Tel.: 81-6-6879-3730; Fax: 81-6-6879-3739; E-mail: ichi@imed2.med.osaka-u.ac.jp.

[1] The abbreviations used are: SST-REX, signal sequence trap by retrovirus-mediated expression screening system; BSA, bovine serum albumin; DMEM, Dulbecco's modified Eagle's medium; FBS, fetal bovine serum; GPI, glycosylphosphatidylinositol; PI, propidium iodide; PIG-A, phosphatidylinositolglycan-class A; PI-PLC, phosphatidylinositol-specific phospholipase C; PNH, paroxysmal nocturnal hemoglobinuria; FITC, fluorescein isothiocyanate; PBS, phosphate-buffered saline; DIG, digoxigenin; CHO, Chinese hamster ovary cells; RT, reverse transcription; ISH, *in situ* hybridization.

by retrovirus-mediated expression screening system) was introduced as described previously by our laboratories (7). Briefly, cDNA was synthesized from the poly(A)$^+$ RNA by random hexamers, using the SuperScript System (Invitrogen), and was then inserted into BstXI sites of the pMX-SST vector, using BstXI adapters (Invitrogen). The ligated DNA was amplified in DH10B cells (Electromax, Invitrogen) to construct an SST-REX library, and a library DNA was prepared using Qiagen plasmid kits (Qiagen). High titer retroviruses representing the SST-REX library were produced using the packaging cell line PlatE and infected to Ba/F3 cells. After 1-day infection period, selection of factor-independent Ba/F3 cells commenced in the absence of interleukin-3, using 96-well multititer plates. The integrated cDNAs were isolated from the interleukin-3-independent Ba/F3 cells by genomic PCR and sequenced.

Animals and Experimental Protocol—C57BL/6J and obese diabetic *db/db* mice were obtained from Clea Japan (Tokyo) and kept under a 12-h/12-h dark/light cycle (lights on: 8 am to 8 pm) at constant temperature (22 °C) with free access to food and water. The composition of the diet was as follows: carbohydrate, 54.0%; protein, 23.8%; and fat, 5.1%. For analysis of intectin mRNA expression in various tissues of mouse, 6-week-old male C57BL/6J mice were used. For fasting and refeeding time-course experiments, 3–4 male mice (6-week-old) were used in each group. The groups consisted of mice fed *ad libitum* with standard chow, mice fasted for 24 h, and mice refed 1, 2, and 4 h after 24-h fasting. Mice were sacrificed under deep anesthesia, and their small intestines were harvested immediately. Experiments designed to determine intectin mRNA expression in the small intestine were conducted in 6-week-old C57BL/6J and *db/db* mice. All experimental protocols described in this report were approved by the Ethics Review Committee for Animal Experimentation of Osaka University.

RNA Isolation, Northern Blot, and Quantitative Reverse Transcription-PCR Analysis—Total RNA was isolated from various tissues, using RNA STAT-60 kit (Tel-Test "B" Inc., Friendswood, TX) according to the instructions provided by the manufacturer.

Ten micrograms of total RNA was subjected to Northern blotting as described previously (8). First strand cDNA was synthesized using ThermoScript™ RT-PCR System (Invitrogen). Quantitative RT-PCR was performed on a LightCycler using the FastStart DNA Master SYBR Green I (Roche Diagnostics, Tokyo, Japan) according to the protocol provided by the manufacturer. The following forward and reverse primers were used for quantitative PCR amplifications: mouse intectin, 5′-GTTGCCCCTGATTCTGCTGG-3′ and 5′-GCACTATTGCAGAGGTCCGT-3′; mouse cyclophilin, 5′-CAGACGCCACTGTCGCTTT-3′ and 5′-TGTCTTTGGAACTTTGTCTGCAA-3′.

Construction of Stable Expression Vector—To express FLAG-tagged intectin, we constructed an expression vector of FLAG-tagged intectin containing the signal sequence of CD59. We prepared a cDNA of intectin (amino acids 21–111: removed the region corresponding to intectin signal sequence) by PCR using a pair of primers containing HindIII and NotI restriction enzyme sites, respectively, 5′-CCCCAAGCTTTTGAAGTGTCATGAATGC-3′, corresponding to amino acids 21–26 and 5′-TTTTTTTTGCGGCCGCCTACTGGCTGAGATAGATATAGC-3′, corresponding to amino acids 106–111. The amplified product was digested with HindIII and NotI to isolate a 290-bp fragment. The pME-puro-FLAG-CD59 vector (a kind gift from Dr. T. Kinoshita, Osaka University) was digested with HindIII-SfiI and NotI-SfiI, respectively. The above three isolated fragments were ligated to generate pME-CD59 (signal sequence)-FLAG-intectin.

Cell Culture—IEC-6 cells were cultured in Dulbecco's modified Eagle's medium (DMEM) supplemented with 10% fetal bovine serum (FBS), 100 units/ml penicillin, and 100 mg/ml streptomycin in a water-saturated atmosphere with 5% CO_2 at 37 °C. To measure palmitate-induced cell death, IEC-6 cells were seeded at a density of 2×10^4 cells/cm^2. The medium was removed 36 h later, and the cells were incubated in DMEM supplemented with 1% FBS in the presence of 0.5% bovine serum albumin (BSA) alone or with various concentrations of palmitate (25, 50, 100, and 200 μM) for 12 h.

Establishment of Stable Cell Lines Expressing FLAG-tagged Intectin—To create stable cell lines that express FLAG-tagged intectin, electroporation was performed using GenePulser transfection apparatus (Bio-Rad Laboratories, Richmond, CA). IEC-6 cells (80–90% confluence) were trypsinized and suspended in DMEM. Approximately 6×10^6 cells were resuspended in FBS-free DMEM without antibiotics and with 10 μg of plasmid DNA in a final volume of 400 μl. Electroporation was performed at room temperature (500 microfarads, 250 V, 0.4-cm cuvette). After electroporation, the cells were incubated at room temperature for 10 min, diluted in DMEM with 10% FBS, and then plated onto a 10-cm dish. The transfected cells were selected by growth in a medium containing 2 μg/ml puromycin. Cell clones were obtained from individual puromycin-resistant colonies using the limiting dilution method. FLAG-tagged intectin expression was investigated by flow cytometry.

Cell Fractionation and Western Blotting—IEC-mock cells (IEC-mock) and IEC-6 cells expressing FLAG-tagged intectin (IEC-intectin) were harvested after confluence. The cells were lysed with extraction buffer containing a protease inhibitor mixture as described previously (8) and divided into membrane fraction and cytosolic fraction by centrifugation (15 min, 20,000 × *g*, 4 °C). Equal amounts of protein were subjected to SDS-14% PAGE and transferred onto polyvinylidene difluoride membrane. The membrane was incubated with a mouse anti-FLAG M2-horseradish peroxidase conjugate (Sigma). Immunoreactive protein bands were visualized by using the ECL kit (Amersham Biosciences).

Flow Cytometry—For selection of FLAG-tagged intectin-expressing cells, cells were stained with anti-FLAG FITC-conjugated antibody. Stained cells were analyzed by FACSort (BD Biosciences). The cellular DNA content was determined by flow cytometric measurement of propidium iodide (PI) binding. In preparation for flow cytometry, both adherent and unattached cells were harvested and combined. The cells were washed twice with ice-cold PBS and fixed with 70% cold ethanol. After treatment with 1 μg/ml DNase-free RNase A in PBS containing 10 μg/ml PI, the cells were analyzed using a FACSort. The cell cycle distribution was quantified by using FlowJO (Tree Star Inc., Ashland, OR) software.

In Situ Hybridization—According to the instructions supplied by the manufacturer (digoxigenin (DIG) RNA labeling kit (SP6/T7), Roche Diagnostics), DIG-labeled RNA probes were synthesized using intectin full-length cDNA, which was cloned into pCRII-TOPO (Invitrogen). Male C57BL/6Cr Slc mice (6-week-old, SLC, Shizuoka, Japan) were deeply anesthetized by sodium pentobarbital and perfused transcardially with PBS and 4% paraformaldehyde in phosphate buffer. Tissues were postfixed for 12–24 h with the same fixative and embedded in paraffin. Tissue sections (4 μm) were treated with 0.2 N HCl for 30 min and 10 μg/ml proteinase K for 15 min at 37 °C followed by re-fixation with 4% paraformaldehyde. Hybridization was performed overnight at 50 °C in a hybridization solution (40% formamide, 0.6 M NaCl, 10 mM Tris-HCl, pH 7.4, 1 mM EDTA, 1× Denhardt's solution, 250 μg/ml tRNA, 125 μg/ml salmon sperm DNA, 10% dextran sulfate, and 200 ng/ml DIG-labeled probe). After treatment with 20 μg/ml RNase A (Sigma) for 30 min at 37 °C, the sections were washed with 0.2× SSC at 55 °C. The sections were immunolabeled with anti-DIG alkaline-phosphatase conjugate (Roche Diagnostics), and color was developed using nitro blue tetrazolium/BCIP (5-bromo, 4-chloro, 3-indoylphosphate), which created black and purple signals. Some specimens were counterstained with hematoxylin.

Cell Viability Assay—The cells (5×10^3/well) in 96-well plates were cultured for 12 h, then exchanged with medium in the absence or presence of various concentrations of apoptotic inducer, and further incubated for 12 h (palmitate) or 24 h (camptothecin and daunorubicin). The cell viability was determined using Cell Count Reagent SF (Nacalai Tesque, Japan). WST-8 (9), which is based on colorimetric quantification of NADH, was added to the culture. After 1 h, absorbance at 450 and 650 nm was measured using a Viento multi-spectrophotometer (Dainippon, Tokyo, Japan).

In Vitro Caspase-3 Activity Assay—Caspase-3 activity was measured using the ApoAlert caspase assay kit (BD Biosciences), using the instructions supplied by the manufacturer. Briefly, cells were washed twice with ice-cold PBS, lysed for 10 min on ice with cell lysis buffer (BD Biosciences), and centrifuged (10 min, 15,000 × *g*, 4 °C) to remove debris. After determination of protein concentration using the BCA protein quantification kit (Pierce Chemical Co.) with BSA as a standard, 10 μg of the protein was incubated with caspase-3 substrate, ac-DEVD-7-amino-4-trifluoromethyl coumarin at 37 °C for 1 h. The initial rate of release of free ac-DEVD-7-amino-4-trifluoromethyl coumarin was measured using a Spectra MAX GeminiXS microplate reader (Molecular Devices, Sunnyvale, CA) in fluorescence mode using an excitation filter of 400 nm and an emission filter of 505 nm. Enzyme activity was calculated according to the formula provided by the manufacturer.

Cell Aggregation Assay—Cell aggregation assay was performed as described previously (10). Parental Chinese hamster ovary (CHO) cells and intectin-transfected CHO cells (CHO-intectin) were washed with PBS and incubated with 0.125% trypsin and 0.5 mM EDTA at 37 °C for 3 min. Dispersed cells were suspended in Hanks' balanced salt solution (1×10^6 cells/ml) and then placed on BSA pre-coated 24-well plate (0.5 ml). The cells were incubated under continuous shaking at 70 rpm for the indicated periods of time. The reaction was stopped with the addi-

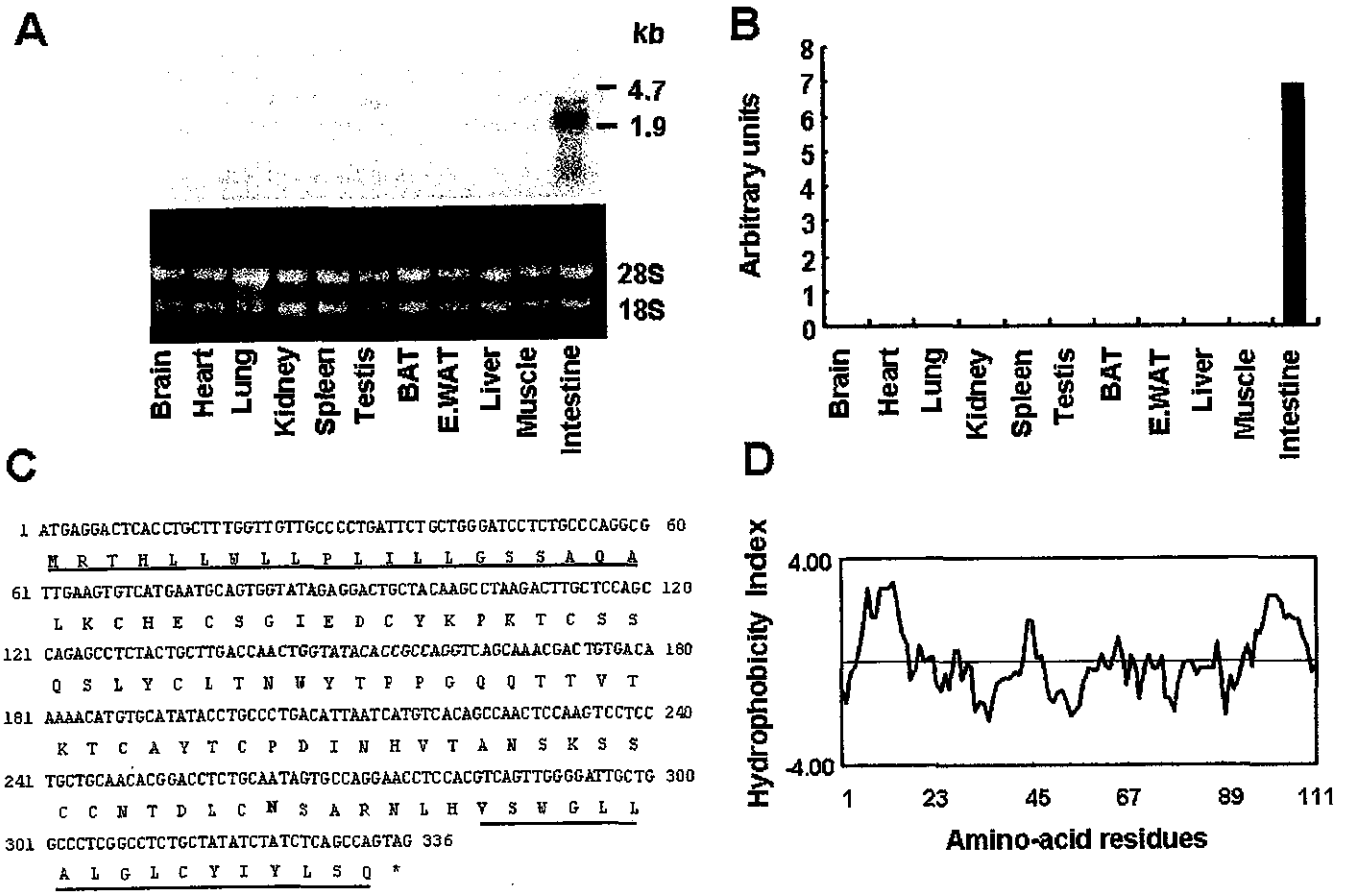

FIG. 1. **Expression and sequence of intectin.** *A*, Northern blot analysis of intectin expression in various tissues of C57BL/6J mice. *B*, quantitative RT-PCR analysis of intectin mRNA expression in various tissues of C57BL/6J mice. *C*, nucleotide and deduced amino acid sequence of intectin. Putative N- and C-terminal signal sequences are *underlined*, and the potential GPI-anchoring site is Asn-88 (*N*) (*bold*). *D*, hydropathy profiles of intectin drawn by using the Kyte and Doolittle program (11).

tion of an equal volume of 4% paraformaldehyde. Samples were evaluated by counting single cells and aggregates.

Statistical Analysis—Data are expressed as means ± S.E. Statistical analyses were performed with unpaired *t*-tests. A p value less than 0.05 denoted the presence of a statistically significant difference.

RESULTS

Identification of Intectin as a Small Intestine-derived Nutritionally Modulated Membrane Protein—We previously developed an efficient SST method using retrovirus-mediated gene transfer (7). To identify small intestine-derived nutritionally modulated membrane protein or secretory protein, we conducted this SST method using the pooled poly(A)$^+$ RNA from the small intestinal epithelium of mice at *ad libitum*, fasted and refed conditions, and obese diabetic *db/db* mice. We screened and sequenced 1224 clones. Four clones were selected as unknown proteins with signal sequence or transmembrane region. The mRNA of one clone was exclusively expressed in the small intestine among various tissues of mice as revealed by Northern blotting analysis and quantitative RT-PCR (Fig. 1, *A* and *B*). This clone and its full-length cDNA were selected and named intectin. The nucleotide sequence and deduced 111-amino acid sequence of intectin are shown in Fig 1*C*. A hydrophobicity plot revealed a 20-residue N-terminal and a 13-residue C-terminal signal peptide (Fig. 1, *C* and *D*) (11). A potential GPI-anchoring site was identified at Asn-88 based on the published GPI consensus sequences (Fig. 1*C*) (12). A Basic Local Alignment Search Tool (BLAST) search revealed that intectin sequence is identical to NM_025929 (GenBank™), whose function is totally unknown, and that intectin has a Ly-6 domain (Fig. 2). All cysteine residues highly conserved among Ly-6 family are present in intectin. The amino acid similarity of intectin to other Ly-6 family is not high, with homology of only 30–40% (Fig. 2).

We established a stable cell line that expressed intectin by transfecting the intectin-FLAG gene into a normal intestinal epithelial cell line, IEC-6. Expression of intectin protein in intectin-transfected IEC-6 (IEC-intectin) and mock-transfected IEC-6 (IEC-mock) are shown in Fig. 3*A*. IEC-intectin cells expressed intectin protein in the cell membrane fraction, and intectin protein was not detected in the cytosolic fraction (Fig. 3*A*). These results suggest that intectin can be considered a membrane-associated protein. As described above, intectin protein has a predicted GPI-anchoring site in Asn-88. To clarify whether intectin is a GPI-anchored protein, we treated the cells with phosphatidylinositol-specific phospholipase C (PI-PLC) exhibiting activity to excise GPI-anchored region. Without PI-PLC treatment, IEC-intectin cells exhibited higher FITC signal on cell membrane, compared with IEC-mock cells (Fig. 3*B*). PI-PLC treatment of IEC-intectin cells decreased the signal to the level of IEC-mock cells (Fig. 3*B*). The same results were observed in FLAG-tagged intectin-transfected CHO cells as well as FLAG-tagged CD59, a known GPI-anchored protein, transfected CHO cells (data not shown). These results indicate that intectin is a GPI-anchored protein.

Exclusive Expression of Intectin in the Small Intestine—Analysis of various tissues of 6-week-old C57BL/6J mice by Northern blotting and quantitative RT-PCR showed that intectin mRNA was expressed exclusively in the small intestine (Fig. 1, *A* and *B*). Unlike other known members of the Ly-6 family, which are highly expressed in peripheral blood leuko-